Kinetic theory of alpha particles production in a dense and strongly magnetized plasma

Carlo Cereceda, Claude Deutsch, Michel De Peretti, Michel Sabatier, Mikhail M. Basko, Andreas Kemp, and Jurgend Meyer-ter-Vehn

Citation: Physics of Plasmas (1994-present) **7**, 4515 (2000); doi: 10.1063/1.1308564
View online: http://dx.doi.org/10.1063/1.1308564
View Table of Contents: http://scitation.aip.org/content/aip/journal/pop/7/11?ver=pdfcov
Published by the AIP Publishing

Kinetic theory of alpha particles production in a dense and strongly magnetized plasma

Carlo Cereceda[a] and Claude Deutsch
LPGP,[b] Bât. 210, UPS, 91405-Orsay, France

Michel De Peretti and Michel Sabatier
CEN-B3, BP 12, 91680-Bruyères-Le-Chatel, France

Mikhail M. Basko,[c] Andreas Kemp, and Jurgend Meyer-ter-Vehn
MPIQ, 85748 Garching, Germany

(Received 4 August 1999; accepted 17 July 2000)

In connection with fundamental issues relevant to magnetized target fusion, the distribution function of thermonuclear alpha particles produced *in situ* in a dense, hot, and strongly magnetized hydrogenic plasma considered fully ionized in a cylindrical geometry is investigated. The latter is assumed in local thermodynamic equilibrium with Maxwellian charged particles. The approach is based on the Fokker–Planck equation with isotropic source S and loss s terms, which may be taken arbitrarily under the proviso that they remain compatible with a steady state. A novel and general expression is then proposed for the isotropic and stationary distribution $f(v)$. Its time-dependent extension is worked out numerically. The solutions are valid for any particle velocity v and plasma temperature T. Higher order magnetic and collisional corrections are also obtained for electron gyroradius larger than Debye length. $f(v)$ moments provide particle diffusion coefficient and heat thermal conductivity. Their scaling on collision time departs from Braginski's. © *2000 American Institute of Physics.* [S1070-664X(00)00211-1]

I. INTRODUCTION: MAGNETIZED TARGET FUSION

The fundamental motivation for magnetizing a pellet a few centimeters in diameter with thermonuclear deuterium–tritium (DT) fuel in it, essentially lies in the drastic reduction of alpha particle and thermal losses when an azimuthal magnetic field **B** (Fig. 1) is superimposed on the independently compressed target.[1,2] The given compression may then be driven at a much lower pace (cm/s) than in usual pellets used for inertial confinement fusion (ICF).

The stagnation period reached when expansion pressure and target compression compensate each other lasts about 10^{-7}–10^{-8} s.

Magnetized target fusion (MTF) is ICF with a magnetic field introduced into the DT fuel. The role of the magnetic field is to reduce the heat conduction losses from the DT plasma and to retain the 3.5 MeV alpha particles. The direct impact of the magnetic pressure on the implosion hydrodynamics and duration of the stagnation phase is typically negligible.

The MTF concept has been discussed in the literature, mostly in the context of spherical implosions,[1–6] and to a lesser extent for cylindrical geometry.[7–9] In this paper we focus our attention on the magnetized DT cylinders. The interest for a cylindrical MTF stems from the following. First, cylindrical geometry is generally better suited for introduction of an external magnetic field. In addition, strong motivation comes from the inertial fusion driven by the beams of heavy ions. For relatively rigid ion beams, which are accelerated, stored and transported along extended horizontal structures, a cylindrical symmetry of target irradiation may be easier to achieve than the spherical one. Ion driven magnetized cylindrical targets could possibility be even envisaged in direct drive schemes for inertial fusion energy.[7]

In the context of the ignition physics, the introduction of a magnetic field into ICF targets lowers the threshold value of the fuel ρR at ignition. This is necessitated by the cylindrical geometry itself because, under similar constraints on the drive pressure uniformity and the Rayleigh–Taylor instability, the cylindrical implosions are less efficient in compressing the fuel than the spherical ones.[9] Also by lowering the fuel ρR at ignition one can reduce considerably the required driver power—a particularly sensitive issue for a heavy ion driver.

Less extreme scenarii include the compression of much larger preinjected plasmas (see Fig. 2 and Table I) of cigarlike shapes with the aid of a field reversed configuration (FRC). Additional and distinct compression histories are certainly possible, provided they share the same initial and final plasma states defined as follows.

The initial plasma density is $\sim 10^{17}\,\mathrm{cm}^{-3}$ at 100 eV temperature and 100 kG while it ends near $10^{20}\,\mathrm{cm}^{-3}$ at peak compression after a few μs compression at 10 keV temperature with $B \leqslant 10\,\mathrm{MG}$. This regime, intermediate between magnetic confinement (tokamaks) and ICF features an electron gyrofrequency much higher than electron collision frequency ($\omega_{ce} \gg \nu_e$) with electron collision time τ_e fulfilling

[a]Present address: Departamento de Fisica, Universidad Simón Bolivar, Apdo. 89000, Caracas, Venezuela.
[b]Associé au CNRS.
[c]On leave from the Institute for Theoretical and Experimental Physics, B. Cheremushkinskaya, Moscow 117259, Russia.

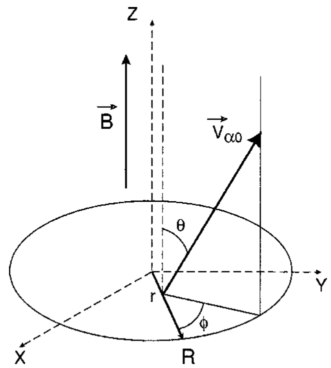

FIG. 1. The coordinate system used in Sec. II for calculating the alpha energy deposition fraction f_α.

$\omega_{ce}\tau_e \gg 1$. Corresponding gyroradii remain much larger than their screening (Debye) length counterpart, so $\lambda_{D\beta} \ll \rho_{L\beta}$ remains valid during compression for every plasma species $\beta(e,i)$. Such a situation is markedly different from magnetic confinement[10] with $\lambda_{D\beta} \gg \rho_{L\beta}$, which implies a basic reformulation of kinetic theory in a very strongly magnetized plasma.[11]

In this context, a certain amount of trajectographic attention has to be paid to the magnetic configuration at hand through a genuine three-dimensional (3D) high beta code providing a detailed magnetic map. The basic interest of a FRC lies in its easy transferability from one device to another. However, even compressed in the central part of the implosion geometry displayed in Fig. 2, the plasma remains magnetically insulated from the surrounding liner but it is not wholly confined. So, guiding center drifts and direct leaking out at specific locations can occur and significantly compete with the standard α stopping on plasma electrons.

Corresponding investigations lie beyond the scope of the present work. In the FRC situation, it has to be noticed that certain volumes that surround the field-null ''x-points'' at each end of the FRC will act as nonadiabatic scattering centers for the alpha trajectories. There then arises a concern that the alpha particles would be scattered out of the plasma after only a few longitudinal passes. This scattering process could severely limit the total path length for significant energy transfer from alpha particles to plasma by Coulomb collisions.

TABLE I. Representative implosion parameters (FRC, see Fig. 2).[a]

	Reactor-like system	Development-sized system
n-TauDwell	$1e15\ \text{s cm}^{-3}$	$2e14\ \text{s cm}^{-3}$
Liner		
Kappa=spheroid ''b/a''	3	3
Velocity	0.30 cm/μs	0.30 cm/μs
Liner energy	66 MJ	0.53 MJ
Final plasma		
$T_i = T_e$	10 keV	10 keV
Density	$1e20\ \text{cm}^{-3}$	$1e20\ \text{cm}^{-3}$
Liner inside radius	2.32 cm	0.46 cm
Liner inside length	13.9 cm	2.78 cm
Liner final thickness	6.5 cm	1.3 cm
Plasma energy	25 MJ	0.2 MJ
B at wall	9 MG	9 MG
Tau Dwell	10 μs	2 μs
Tau classical heat loss	1410 μs	56 μs
Tau Bohm	35 μs	1.4 μs
Preimplosion plasma		
density	$1e17\ \text{cm}^{-3}$	$1e17\ \text{cm}^{-3}$
Temperature	100 eV	100 eV
Radius	23 cm	4.4 cm
Length	140 cm	27 cm
Liner thickness	0.40 cm	0.07 cm
Plasma energy	750 kJ	7 kJ
B at wall	28 kG	28 kG
Tau classical heat loss	290 μs	12 μs
Tau Bohm	1580 μs	63 μs

[a]After R. E. Siemon, I. R. Lindemuth, and K. F. Schoenberg, in Ref. 1.

Those considerations explain that in the sequel we shall restrict attention to the geometry (Fig. 1) of a uniformly magnetized cylinder at high B values $\sim 10^7 - 10^8$ G in order to secure particle gyroradii much smaller than target transverse dimensions but still fulfilling $\lambda_{D\beta} \ll \rho_{L\beta}$ in view of the high densities envisioned in the stagnating target. Those B values lie within reach of present pulse power technology.

Therefore, the kinetic-theoretic investigations displayed below are likely to bear more relevance to cylindrical targets driven by intense ion beams[7–9] than to linear-compressed spherical ones.[1–6]

As far as α_s' stopping in plasma is concerned, it should

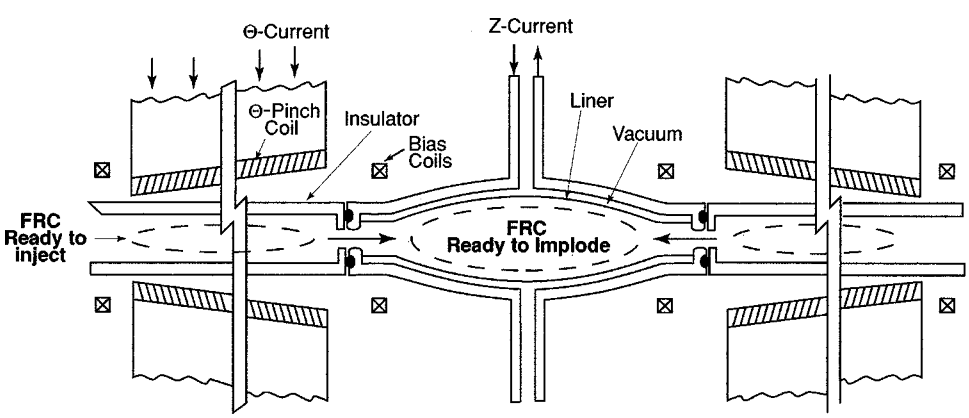

FIG. 2. Field reversed configuration (FRC) plasma in implosion geometry [R. E. Siemon, I. R. Lindemuth, and K. F. Schoenberg, Ref. 1, p. H 1].

be appreciated that it is the product BR (R denotes cylinder radius at stagnation) which matters.

In the sequel, we shall elaborate on the equilibrium time scale t_{eq} for the α particle distribution to relax to equilibrium.

It satisfies $t_{\mathrm{eq}} \sim \tau_{\alpha e}$ (energy exchange time)$=[m/2me]\tau_e$ with electron collision time[10] $\tau_e = (10^6 T_e^{3/2}(\mathrm{eV})\mathrm{s}/2.91 n_e(\mathrm{cm}^{-3}) \ln \Lambda) \cdot (1/Z^2)$. m denotes α particle mass, $Z=2$ and $\ln \Lambda$ is the usual plasma Coulomb logarithm.

The nonthermal component of the α particle one-body distribution function reaches equilibrium rapidly, so $t_{\mathrm{eq\ non\ th}} \sim 10^{-9}\,\mathrm{s} < \tau_{\alpha e}$. Energetically, this is a most significant phenomenon.

The thermonuclear α particles are expected to lose their kinetic energy through inelastic collisions with electrons. Small angle deflections also arise from quasielastic scattering on target plasma ions.

So, as in the tokamak oriented literature,[10,12] it proves convenient to investigate the α_s' particle distribution function (pdf) in a weak collision framework patterned upon the standard Fokker–Planck equation (FPE). Larmor radii remaining larger than Debye lengths the particles curvature within Debye sphere is negligible.

So, it is reasonable to initialize the α_s' pdf with a B-free and velocity (v)-isotropic approximation.

In a tokamak context, it is customary to compute transport quantities through a Maxwell distribution for the fusioning D^+ and T^+ ions. This procedure leads to a realistic expression for the α source term S, isotropic with respect to particle velocities. Recently, Liberman–Velikovich[13] and Cozzani–Horton[14] have obtained equilibrium FPE velocity distribution $f(v)$ for α particles under the proviso

$$v_{Thi} \ll v \ll v_{The}, \qquad \frac{kT_\beta}{mv} \cdot \frac{\partial f}{\partial v} \ll f, \tag{1}$$

where v_{Thi} and v_{The}, respectively, refer to plasma ion and electron thermal velocities, while β is the plasma particles index.

These conditions are easily fulfilled only in high temperature plasmas for high v values.

$f(v)$ is a theoretical object of a paramount conceptual and operational significance, and it is first involved in the time-independent ionic and electronic conductivities used for estimating the energy balance in the igniting target, for instance. Every transport quantity relies on it. Moreover, as well-documented a small density of energetic thermonuclear α particles is able to modify significantly the pressure in the plasma where they are stopped.

From now on this paper is structured as follows:

The energy fraction f_α of thermonuclear α_s' which is really deposited in the target cylinder is estimated in Sec. II altogether with ignition criterion in the MTF scenario.

Standard FPE kinetic theoretic formalism is introduced in Sec. III for a v-isotropic $f(v)$. A novel stationary solution is shown in Sec. IV for arbitrary source term S and loss term s. Connection with results valid when inequalities (1) hold is then discussed. Time-dependent extensions of these solutions are examined in Sec. V. Relaxation to equilibrium is given a specific attention in Sec. VI. Magnetic and collisional higher order corrections to above B-free $f(v)$ are established in Sec. VII. $f(v)$ v-moments leading to various time-independent transport quantities are worked out in Sec. VIII. Finally, a few provisional and prospective remarks are offered as a conclusion in Sec. IX.

II. ENERGY DEPOSITION BY ALPHA PARTICLES (REF. 9)

We consider the energy fraction of the 3.5 MeV alpha particles, f_α, deposited due to the Coulomb collisions with plasma electrons in a uniform magnetized DT cylinder of radius R embedded into a uniform magnetic field B directed along the cylinder axis. The dimensionless quantity $0 < f_\alpha < 1$ is a function of two dimensionless parameters,

$$\overline{R} = \frac{R}{l_\alpha}, \quad c = \frac{R}{\rho_{L\alpha}} = R\frac{\omega_\alpha}{v_{\alpha 0}}, \tag{2}$$

with l_α, the Coulomb range of the alpha particles, $\rho_{L\alpha}$ is their Larmor radius at the birth velocity $v_{\alpha 0} = 1.3 \times 10^9$ cm/s, and

$$\omega_\alpha = \frac{2eB}{m_\alpha c} \tag{3}$$

is their Larmor frequency. We consider the entire variation range of $0 < \overline{R}$, $c < \infty$, with a particular attention for the $\overline{R} \ll 1$.

A. Method of calculation

We assume that the Coulomb collisions decelerate alphas by means of dynamic friction only, and the diffusion in the velocity space can be neglected in the following estimates. The friction force is supposed to be directly proportional to the velocity of alphas, which is a reasonable approximation for plasma temperatures $1\,\mathrm{keV} \leq T \leq 20\,\mathrm{keV}$. Then, the equations of motion for an individual alpha particle become

$$\begin{aligned} \dot{v}_x &= \omega_\alpha v_y - \nu_\alpha v_x, \\ \dot{v}_y &= -\omega_\alpha v_x - \nu_\alpha v_y, \\ \dot{v}_z &= -\nu_\alpha v_z, \end{aligned} \tag{4}$$

where the dot denotes the time derivative,

$$\nu_\alpha = \frac{v_{\alpha 0}}{l_\alpha} \tag{5}$$

is the effective collision frequency of the fast alphas, and the coordinate system is shown in Fig. 1 (the magnetic field B is along the z-axis).

For the deceleration law given by Eqs. (4), the fraction of the initial energy deposited by an individual alpha particle after it travels a distance s is given by

$$f_{\alpha s} = f_{\alpha s}(r,\theta,\phi) = 2\left(\frac{s}{l_\alpha}\right) - \left(\frac{s}{l_\alpha}\right)^2. \tag{6}$$

Here r is the cylindrical radius of the alpha birth point, θ is the pitch angle, and ϕ is the azimuth (in the xy plane, with respect to the radius vector of the birth point) of the alpha birth velocity $\mathbf{v}_{\alpha 0}$ (see Fig. 1). In Eq. (6), $s = s(r,\theta,\phi)$ is the path length of an alpha particle with the birth parameters, r,θ,ϕ before it stops inside the cylinder or leaves it by crossing the boundary at $r=R$. We assume for simplicity that, once an alpha particle exits the cylinder at $r=R$, it never returns. Any attempt to account for the re-entry of gyrating alphas should take into consideration matter distribution outside the cylinder $r=R$, which would be beyond the scope of this work. Equations (4) imply that $s=l_\alpha[1-\exp(-\nu_\alpha t)]$, so one only has to determine by integrating Eqs. (4) the time t at which the particle with the birth parameters r,θ,ϕ exits the cylinder $r=R$.

Once the function $f_{\alpha s}(r,\theta,\phi)$ is known, one calculates f_α by averaging $f_{\alpha s}$ from Eq. (6) over the angles θ,ϕ and the radius r,

$$f_\alpha=\frac{2}{E^2}\int_0^R r\,dr\,\frac{1}{4\pi}\int_0^\pi \sin\theta\,d\theta\int_0^{2\pi} f_{\alpha s}(r,\theta,\phi)=d\phi. \tag{7}$$

B. Asymptotical behavior and numerical results

As a first step, consider the simplest case of $B=0$ ($c=0$), when the absorbed energy fraction f_α is a function of one parameters $\bar{R}=R/l_\alpha$ only. In the case of a uniform sphere of radius R, all the integrals in Eq. (7) can be calculated analytically. Not so for the cylinder; only the asymptotical behavior in the limits of $\bar{R}\ll 1$ and $\bar{R}\gg 1$ can be established analytically,

$$f_\alpha(\bar{R},b=0)=\begin{cases}\frac{8}{3}\bar{R}+0(\bar{R}^2), & \bar{R}\ll 1,\\ 1-\dfrac{1}{6R}+0\left(\dfrac{1}{R^2}\right), & \bar{R}\gg 1.\end{cases} \tag{8}$$

Next, we examine qualitatively the dependence of f_α on the magnetic field strength B in the limit of $R\ll l_\alpha(\bar{R}\ll 1)$. For this, all the alphas born inside the DT cylinder can be roughly divided into two groups, namely, those born at large pitch angles $\theta\sim\pi/2$ (propagating nearly radially), and those born in the narrow ''capture cone'' $0<\theta\leq\theta_c\ll 1$, $0<\pi-\theta\leq\theta_c\ll 1$. When $R\ll\rho_{L\alpha}$, all the ''nearly radial'' alphas escape the cylinder along almost straight trajectories, leaving a small fraction $f_{\alpha s}\sim\bar{R}$ of their initial energy in the DT plasma. The alphas born within the capture cone deposit all their energy in the DT cylinder, so that their contribution to f_α is proportional to the solid angle occupied by the capture cone, i.e., to θ_c^2. The width of the capture cone can be readily evaluated as

$$\theta_c\sim\begin{cases}\dfrac{R}{l_\alpha}, & R\ll l_\alpha\ll\rho_{L\alpha},\\ \dfrac{R}{r_{L\alpha}}, & R\ll\rho_{L\alpha}\ll l_\alpha.\end{cases} \tag{9}$$

As a result, we infer the following asymptotic behavior for the total absorbed energy fraction:

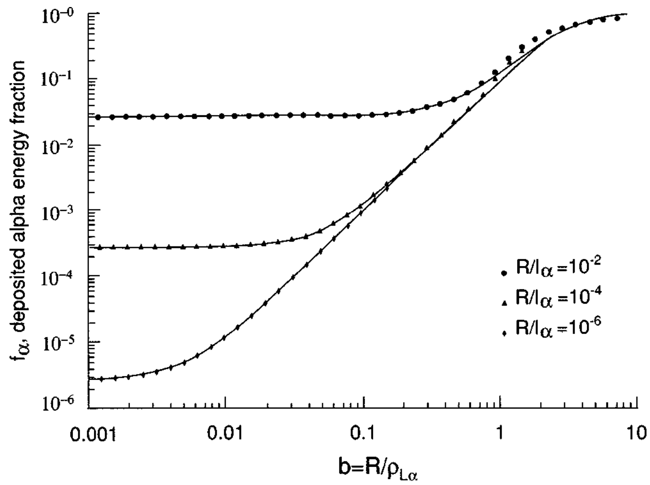

FIG. 3. The energy fraction f_α, which the 3.5 MeV alpha particles deposit in a uniform magnetized DT cylinder, as calculated by performing numerical integration in Eq. (7) (dots, triangles, and diamonds). Approximate formula (12) is plotted with the solid curves. The three curves display the dependence of f_α on the dimensionless parameter c for three different values of $\bar{R}$ [see Eq. (2)].

$$f_\alpha(\bar{R},c)\sim\begin{cases}\frac{8}{3}\bar{R}+0(\bar{R}^2), & R\ll l_\alpha\ll\rho_{L\alpha}(c\ll\bar{R}\ll 1),\\ \frac{8}{3}\bar{R}+0(c^2), & R\ll\rho_{L\alpha}\ll l_\alpha(\bar{R}\ll c\ll 1),\\ 1-0\left(\dfrac{1}{c}\right), & \rho_{L\alpha}\ll R\ll l_\alpha(\bar{R}\ll 1\ll c).\end{cases} \tag{10}$$

In the last limit of a very strong magnetic field, $r_{L\alpha}\ll R$, only a small fraction of alphas born in a narrow surface layer of width $r_{L\alpha}$ escape the DT cylinder.

The dependence of $f_\alpha(R,c)$ on c, calculated by integrating numerically Eq. (10), is shown in Fig. 3 for three different values of $\bar{R}$. These calculations are in full agreement with the asymptotical formulas of Eq. (10). In particular, it is clearly seen that the transition from the ''optically thin'' limit of $f_\alpha\approx\frac{8}{3}\bar{R}\ll 1$ in the nonmagnetized case to a full absorption with $f_\alpha\approx 1$ in the limit of strong magnetization ($c\gg 1$) does indeed proceed through the intermediate value

$$f_\alpha\propto c^2\propto(BR)^2 \tag{11}$$

useful for practical applications.

For practical needs one would prefer to have a simple approximate formula for f_α. It reads as

$$f_\alpha=\frac{x_\alpha+x_\alpha^2}{1+13x_\alpha/9+x_\alpha^2}, \tag{12a}$$

$$x_\alpha=\frac{8}{3}\left(\bar{R}+\frac{c^2}{\sqrt{9c^2+1000}}\right). \tag{12b}$$

For the zero magnetic field ($B=c=0$) this formula conforms to the both limits in Eq. (8), and never deviates from the numerical results by more than 3.5% (for the quantity $1-f_\alpha$ the maximum deviation amounts to 10%). The dependence on c in Eq. (12b) is chosen such as to describe both limits of $c\ll 1$ and $c\gg 1$ as given by Eq. (10), and to fit the numerical results shown in Fig. 3. It has two numerical constants under the square root; the free term 1000 fits the numerical results along the intermediate asymptote (11), while the coefficient 9 by c^2 is chosen on the basis of the diffusion approximation.

C. Ignition criterion for the MTF mode

The well known ICF ignition criterion for the nonmagnetized DT fuel is usually quoted as a lower bound on the fuel T and ρR values. For DT cylinders it reads as[9]

$$T = 5-7 \text{ keV}, \quad \rho R \geqslant 0.2 \text{ g/cm}^2. \tag{13}$$

The MTF ignition mode aims at igniting the DT fuel at ρR values considerably lower than the ICF threshold of 0.2–0.3 g/cm^2. Hence, the constraint on ρR should be replaced by another condition. We find this condition through the thermal balance of stagnating fuel with zero net heating rate

$$c_0 \frac{dT}{dt} = q_{tn} - q_{br} - q_c . \tag{14}$$

Here,

$$c_0 = 1.158 \times 10^{15} \text{ erg g}^{-1} \text{keV}^{-1} \tag{15}$$

is the heat capacity of the equimolar DT mixture,

$$q_{tn} = 8.18 \times 10^{40} \rho \langle \sigma v \rangle_{\mathrm{DT}} f_\alpha [\text{erg g}^{-1} \text{s}^{-1}] \tag{16}$$

is the rate of the thermonuclear heating by the alpha particles,

$$q_{br} = 3.11 \times 10^{23} \rho T_{\mathrm{keV}}^{1/2} [\text{erg g}^{-1} \text{s}^{-1}] \tag{17}$$

is the rate of bremsstrahlung cooling while

$$q_c = \frac{2(\kappa_e + \kappa_i) T}{\rho R^2} \tag{18}$$

denotes heat conduction energy loss. The heat balance equation (14) is written for a DT column surrounded by either a cold liner or a cold dense DT shell at the time of maximum compression, when the power of the PdV work against the hot duel is zero. CGS units are used, and T is given in keV.

Demanding $q_{tn} > q_{br}$, Eqs. (16) and (17) yield

$$f_\alpha > 3.8 \times 10^{-18} \frac{T_{\mathrm{keV}}^{1/2}}{\langle \sigma v \rangle_{\mathrm{DT}}}, \tag{19}$$

with a right-hand side reaching a minimum 3.1×10^{-2} value at $T = 40$ keV. This highlights the interest of this mode for D–He^3 burns.

Restricting to the more usual $T \approx 7-10$ keV range, Eq. (19) yields

$$f_\alpha > 0.25 - 0.1. \tag{20}$$

From Fig. 3 we infer that, in the limit of $R \ll l_\alpha$, inequality (20) implies a lower bound on the parameter

$$c = \frac{R}{\rho_{L\alpha}} > 1.5 - 1.0, \tag{21}$$

or, equivalently, a lower bound on the product BR. In other words, ignition in the MTF regime requires the 3.5 MeV alpha particles to be at least marginally magnetized, so that their Larmor radii be at least about equal to the hot fuel radius R.

Adding the conduction cooling,

$$q_c = \frac{2\kappa_i T}{\rho R^2} = 1.145 \times 10^{24} \frac{\rho T_{\mathrm{keV}}^{1/2}}{c^2} [\text{erg g}^{-1} \text{s}^{-1}], \tag{22}$$

to the ignition condition

$$q_{tn} > q_{br} + q_c ,$$

we obtain

$$f_\alpha > 3.8 \times 10^{-18} \frac{T_{\mathrm{keV}}^{1/2}}{\langle \sigma v \rangle_{\mathrm{DT}}} \left(1 + \frac{3.68}{c^2} \right). \tag{23}$$

In the limit of $R \ll l_\alpha$, when f_α becomes a function of c only in the relevant parameter range, inequality (23) yields

$$c > 2.3 - 1.5 \tag{24}$$

(for temperature $T = 7-10$ keV). Finally, we reach the ignition criterion for magnetized cylindrical targets

$$T = 7-10 \text{ keV}, \quad BR \geqslant (6.5 - 4.5) \times 10^5 \text{ G cm}, \tag{25}$$

which replaces the ICF criterion (13). Conditions (25) must be fulfilled in the DT fuel at stagnation if the ignition is to occur at a ρR value significantly below the ICF threshold of 0.2–0.3 g/cm^2.

Inequality (23) implies that there is no regime with $q_c \gg q_{br}$; the bremsstrahlung is always at least comparable to (if not larger) the heat conduction as a cooling mechanism near the ignition threshold of magnetized targets.

III. VELOCITY DISTRIBUTION $f(v)$ OF THERMONUCLEAR α PARTICLES

A. Time scales

As usual in a kinetic approach, one expects that a characteristic hydrodynamic time $\tau_0 \sim L/C_s$ (with L typical of plasma extension and isothermal sound speed C_s) remains much larger than the $f(v)$ relaxation time $\tau_1 \sim l_{\mathrm{MFP}}/\langle v \rangle$, in terms of the α_s' mean free path l_{MFP} and thermalized velocity $\langle v \rangle \sim \sqrt{T/m}$.

One also assumes $L \gg l_{\mathrm{MFP}}$, so $f(v)$ relaxes much more rapidly to equilibrium than hydrodynamics, i.e., $\tau_1 \ll \tau_0$.

Moreover, a characteristic time for α particles to travel a screening distance in the hosting plasma is $\tau_2 \sim \lambda_D/\langle v \rangle$.

From $\tau_1 \cong 1/\nu$ and $\tau_2 \cong 1/\omega_p$, one can, respectively, derive the electron collision frequency ν and plasma frequency ω_p. The high temperature albeit dense thermonuclear plasmas of present interest are weakly coupled with a large number of particles $N = n\lambda_D^3 \gg 1$, in the Debye sphere with $\omega_p \gg \nu (\tau_2 \ll \tau_1)$.

B. Fokker–Planck equation (FPE)

Neglecting any bound state effect in a fully ionized hot plasma as well as any recombination or excitation process, one can implement standard kinetic-theoretic procedures reviewed by Sivukhin[15] to establish the relevant FPE, which reads as (repeated index implies summation)

$$\frac{\partial f}{\partial t}+v_i\frac{\partial f}{\partial r_i}+\frac{1}{m}\frac{\partial}{\partial v_i}(X_i f)=\frac{\partial j_i}{\partial v_i} \tag{26}$$

for α particles (mass m, charge q) in presence of a self-consistent electromagnetic force $\mathbf{X}$ while

$$j_i=a_i f-\frac{d_{ij}\partial f}{\partial v_j} \tag{27}$$

denotes particle flux in v-space in the presence of collisions. In the right-hand side of Eq. (27), we have friction vector $\mathbf{a}$ with components

$$a_i=\frac{2\pi}{m}\left(\frac{qq^*}{4\pi\epsilon_0}\right)^2 L\int u_{ij}\frac{\partial f^*(V^*)}{\partial v_j}d^3v^* \tag{28}$$

(* is a species index equivalent to former β) and diffusion tensor d with components

$$d_{ij}=\frac{2\pi m^*}{m^2}\left(\frac{qq^*}{4\pi\epsilon_0}\right)^2 L\int u_{ij}f^*(v^*)d^3v^*, \tag{29}$$

in terms of the distribution $f^*(v^*)$ for species $*$ interacting with the test α-particles. L refers to the usual Coulomb logarithm

$$L=\ln\Lambda_\beta\cong\ln\frac{\lambda_D^*}{r_0^*}$$

with species Landau length $r_0^*=qq^*/4\pi\epsilon_0 T^*$ in terms of electric charges q and q^*, while

$$u_{ij}=\frac{u^2\delta_{ij}-u_iu_j}{u^3}=\frac{\partial^2 u}{\partial u_i\partial u_j}.$$

When test particles α with unknown f experiences collisions with particle species $*$ taken at equilibrium with Maxwell distribution

$$f^*(v^*)=n^*\left(\frac{b^*}{\sqrt{n}}\right)^3 e^{-b^*v^{*2}},\quad b^*=\sqrt{\frac{m^*}{2T^*}},$$

expression (4) becomes

$$a_i=-\frac{4\pi n^*L}{mm^*v^3}\left(\frac{qq^*}{4\pi\epsilon_0}\right)^2\phi_1(b^*v)v_i, \tag{30}$$

where

$$v_jd_{ij}=-\frac{m^*}{2mb^{*2}}a_i$$

and

$$\phi_1(x)=\phi(x)-x\frac{\partial\phi(x)}{\partial x}, \tag{31}$$

while $\phi(x)$ denotes the error function

$$\phi(x)-\frac{2}{\sqrt{\pi}}\int_0^x e^{-t^2}dt. \tag{32}$$

So,

$$\phi_1(x)=\frac{2}{\sqrt{\pi}}\int_0^{x^2}e^{-y}\sqrt{y}dy. \tag{33}$$

Now, we have to take care that the α particles are produced in a finite region, where they spend a limited amount of time. So, in the right-hand side of the FPE (26), we have to add a source S and a loss s. At thermonuclear temperatures, target ions enjoy an isotropic Maxwellian distribution.

Let us consider plasma ions from species a and b with[12]

$$f_i(v)=n_i\left(\frac{m_i}{2\pi T_i}\right)^{3/2}e^{-(m_iv^2/2T_i)}, \tag{34}$$

experiencing fusion reaction $a+b\to\alpha+d+Q(Q>0)$.

According to Kolesnichenko,[12] the corresponding reaction efficiency is expressed as (σ denotes thermonuclear cross-section)

$$\epsilon_{ab}\frac{n_an_b}{8\pi}\left(\frac{m_am_b}{4\pi^2T^2}\right)^{3/2}|\mathbf{v}_a-\mathbf{v}_b|\sigma$$
$$\times e^{-(m_av_a^2/2T)-(m_bv_b^2/2T)}d^3v_ad^3v_bd\Omega, \tag{35}$$

in terms of velocities $\mathbf{v}_a$ and $\mathbf{v}_b$ for particles a and b (resp.), while particle α exits in solid angle $d\Omega$ with $\epsilon_{ab}=0.5$ for the D–D reaction and 1 for the D–T reaction.

Expressing relative velocity in terms of center of mass (cm) velocity v_{cm}, and keeping track of the energetic balance $\mu=[m_am_b/(m_a+m_b)]$,

$$\frac{\mu v^2}{2}+Q=\frac{(m_a+m_b)m}{2m_d}(v-v_{\mathrm{cm}})^2, \tag{36}$$

expression (11) may be integrated in, v-space, which makes to appear the sought for source term as the $\alpha_s' f(v)$ which reads as (E_α=initial α kinetic energy)

$$S(v)=\frac{\dot{n}_\alpha}{4\sqrt{2}\pi^{3/2}v_av_{Thi}v}\{e^{[(v-v_a)^2/2v_{Thi}^2]}$$
$$-e^{[(v+v_a)^2/2v_{Thi}^2]}\},\quad v_a=\sqrt{\frac{2E_a}{m_a}}, \tag{37}$$

with production rate

$$\dot{n}_\alpha=n_{i1}n_{i2}\langle\sigma v\rangle, \tag{38}$$

with $n_{i\beta}$, ion density species β and $\langle\sigma v\rangle$, averaged over the Maxwell distribution (34). To ease future manipulations, it proves convenient to introduce a dimensionless electron velocity $u=bv$, with $b=\sqrt{m_e/2T_e}$. So, expression (37) becomes a bit simpler when expressed as

$$S(u)=\frac{\dot{n}_\alpha b^3\sqrt{\gamma}}{4\pi^{3/2}u_au}\{e^{-\gamma(u-u_a)^2}-e^{-\gamma(u+u_a)^2}\},\quad \gamma=\frac{m_i}{m_e}. \tag{39}$$

At this juncture, it appears highly plausible to initialize f with a v-isotropic expression $f=f(\mathbf{r},v,t)$. Then using

$$\frac{\partial f(v)}{\partial v_i}=\frac{v_i}{v}\frac{\partial f(v)}{\partial v},\quad v=\sqrt{\sum v_i^2},$$

one can now expand the right-hand side of the FPE (26) with

$$-\sum_\beta \frac{\partial j_i}{\partial v_i}+S-s=\sum_\beta C_\beta \frac{\partial}{\partial v_i}\left(\frac{\phi_{1\beta} v_i}{v^3} f\right)+\frac{C_\beta T_\beta}{m} \frac{\partial}{\partial v_i}\left(\frac{\phi_{1\beta} v_i}{v^4} \frac{\partial f}{\partial v}\right)+S-s, \tag{40}$$

and restored β notation for species index in the plasma. For instance,

$$\phi_{1\beta} \text{ is } \phi_1(b_\beta v), \quad b_\beta=\sqrt{\frac{m_\beta}{2T_\beta}}, \tag{41a}$$

and

$$C_\beta=\frac{4\pi n_\beta}{m m_\beta}\left(\frac{q q_\beta}{4\pi\epsilon_0}\right)^2. \tag{41b}$$

Working out derivatives and sums, one obtains

$$-\frac{\partial j_i}{C_\beta \partial v_i}=3\frac{\phi_1}{v^3}+\frac{v_i^2}{v}\frac{\partial}{\partial v}\left(\frac{\phi_1}{v^3}\right)+\left[\frac{\partial}{\partial v_i}\left(\frac{\phi_1 v_i}{v^3}\right)\right] f+\frac{\phi_1 v_i}{v^3}\frac{\partial f}{\partial v_i}+\frac{T_\beta}{m}\left\{\frac{\phi_1}{v^4}+\frac{v_i^2}{v}\frac{\partial}{\partial v}\left(\frac{\phi_1}{v^4}\right)+\frac{\partial}{\partial v_i}\left(\frac{\phi_1 v_i}{v^4}\right)\frac{df}{dv}+\frac{\phi_1 v_i^2}{v^5}\frac{\partial}{\partial v}\left(\frac{\partial f}{\partial v}\right)\right\}, \tag{42}$$

with β implicit in ϕ_1. Then for an isotropic *f*, the corresponding FPE may be formalized as

$$\frac{df}{dt}=\sum_\beta \frac{C_\beta}{v^2}\frac{\partial}{\partial v}\left(\phi_{1\beta} f+\frac{T_\beta}{m}\frac{\phi_{1\beta}}{v}\frac{\partial f}{\partial v}\right)+S-s, \tag{43}$$

with the left-hand side featuring total time *f* variation.

C. FPE with $S\neq 0$

To the best of our knowledge, we are not aware of any general solution available for Eq. (43), when $S\neq 0$. If $S=0$, *f* emerges as a maxwellian. Former attempts[13,14,16,17] have simplified the issues by restricting to inequalities (1). In this framework, Eq. (43) is approximated by

$$\frac{df}{dt}\cong\frac{2}{\tau_{\alpha e}}\frac{\partial}{\partial v_i}(v_i f)+\frac{m_i v_c^3}{m\tau_{\alpha e}}\frac{\partial}{\partial v_j}\left(V_{jk}\frac{\partial f}{\partial v_k}+\frac{2m v_j}{m_i v^3} f\right)+S-s, \tag{44}$$

where $V_{jk}=(v^2\delta_{jk}-v_j v_k)/v^3$. v_c refers to a projectile (α particle) velocity so that electron and ion collisions produce same energy loss, so that

$$v_c^3=\frac{3\sqrt{\pi} m_e}{\sqrt{2} m_i} v_{The}^3. \tag{45}$$

Usually,[13,14] thermalized particles are considered as lost ones. So, one may use a loss function[14] under the form

$$s(v)=0, v>v_{\text{cutoff}}, \quad v_{\text{cutoff}}\sim 3v_{Thi}/2. \tag{46}$$

Simplifying as above the right-hand side of Eq. (44), one gets

$$\frac{\tau_{\alpha e}}{2}\frac{df}{dt}\cong\frac{\partial}{\partial v_i}(v_i f)+\frac{m_i v_c^3}{2m}\frac{\partial}{\partial v_j}\times\left(\frac{v^2\delta_{jk}-v_j v_k}{v^3}\frac{\partial f}{\partial v_k}+\frac{2m v_j}{m_i v^3} f\right)+\frac{S\tau_{\alpha e}}{2}\cong 3f+\left(v+\frac{v_c^3}{v^2}\right)\frac{\partial f}{\partial v}+\frac{S\tau_{\alpha e}}{2} \tag{47}$$

while neglecting second order derivatives. This simplified equation is valid only for nonthermal α_s' with isotropic *f*. Introducing $u=bv$ in Eq. (47) one obtains

$$0\cong 3f+\left(u+\frac{u_c^3}{u^2}\right)\frac{df}{du}+\frac{S\tau_{\alpha e}}{2}, \quad u_c^3\equiv b^3 v_c^3=\frac{1}{p\gamma}, \tag{48}$$

where

$$p=\frac{4}{3\sqrt{\pi}}, \quad \gamma=\frac{m_i}{m_e},$$

satisfied by

$$f\cong-\frac{\tau_{\alpha e}}{2(u^3+u_c^3)}\int S u^2 du. \tag{49}$$

Taking the $E_\alpha/T\to\infty$ limit of the source term (37), one has

$$S\cong\frac{\dot n_\alpha b^3\delta(u-u_\alpha)}{4\pi u_\alpha^2}, \tag{50}$$

which leads to

$$f\cong\frac{\dot n_\alpha \tau_{\alpha e} b^3\theta(u_\alpha-u)}{8\pi(u^3+u_\alpha^3)}, \tag{51}$$

where

$$\theta(x)=\begin{cases}0, & x<0\\ 1, & x>0.\end{cases}$$

In the sequel, it will be practical to work with dimensionless distributions $F\equiv f/n_\alpha\tau_{\alpha e} b^3$. The corresponding normalized expression thus reads

$$F\cong\frac{p\gamma\theta(u_\alpha-u)}{8\pi(p\gamma u^3+1)}, \tag{52}$$

which is pictured in Fig. 4.

IV. STATIONARY FPE SOLUTION

Actually, it is not so difficult to work out a *t*-independent solution of the foregoing FPE when $S-s\neq 0$. Again, restricting to isotropic *f*, Eq. (43) provides an easily tractable stationary limit with

$$\frac{\partial}{\partial v}\left(Mf+\frac{N}{m}\frac{1}{v}\frac{\partial f}{\partial v}\right)=-(S-s)v^2 \tag{53}$$

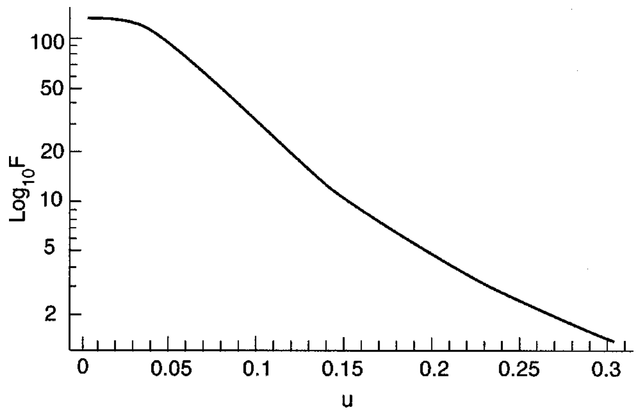

FIG. 4. Approximate and dimensionless solution of the simplified FPE for $E_\alpha=3.5$ MeV, $T=5$ keV$\rightarrow u_\alpha=0.308$.

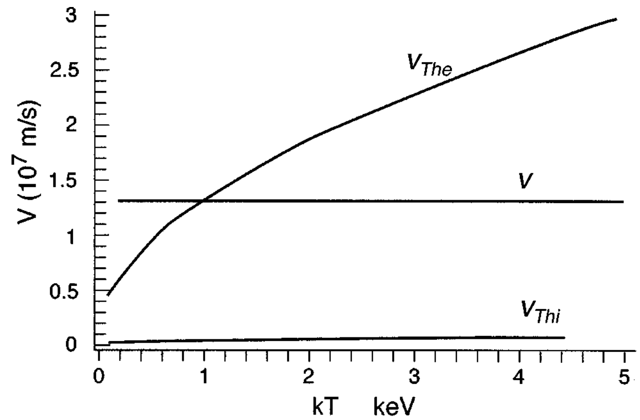

FIG. 5. Mean initial α-particle velocity v contrasted to v_{The} and v_{Thi} in terms of $T=T_e=T_i$.

with

$$M=\sum_\beta C_\beta\phi_{1\beta} \quad \text{and} \quad N=\sum_\beta C_\beta\phi_{1\beta}T_\beta.$$

As already suggested, one also expects the boundary condition $f(v_l)=0$, $v_l\gg v_\alpha$, recalling that v_α is the α particles creation velocity and that they lose it to the hosting plasma. Moreover, when $V\leqslant V_{Thi}$, the thermonuclear particles get thermalized and turn Maxwellian, while fulfilling $\partial f/\partial v|_{v=0}=0$. With those two boundary conditions, one can transform Eq. (53) by integrating once with respect to V, which yields

$$Mf+\frac{N}{m}\frac{1}{v}\frac{\partial f}{\partial v}=-\int (S-s)v^2dv, \tag{54}$$

with a solution for the homogeneous part

$$f_h=f_{h0}e^{-m\int M/Nv dv}. \tag{55}$$

A full solution is then available by looking for a v-dependence,

$$f_h(v)=f_{h0}(v)e^{-m\int M/Nv dv}, \tag{56}$$

and Eq. (54) becomes

$$\frac{N}{m}\frac{1}{v}\frac{\partial f_{h0}(v)}{\partial v}e^{-m\int M/Nv dv}=-\int (S-s)v^2dv+C_1, \tag{57}$$

fulfilled by

$$f_{h0}=m\int \frac{ve^{m\int^v M/Nv'dv'}(-\int^v(S-s)v'^2dv'+C_1)}{N}dv +C_2. \tag{58}$$

Finally, a general equilibrium solution for arbitrary S and s may be expressed under the form

$$f(v)=me^{m\int^v M/Nv'dv'} \times\int \frac{ve^{m\int^v M/Nv'dv'}(-\int^v(S-s)v'^2dv'+C_1)}{N}dv +C_2e^{-m\int^v M/Nv'dv'}. \tag{59}$$

The first boundary condition demands $C_2=0$, recalling that a Maxwellian can vanish only at infinity.

So, one is left with

$$f(v)=me^{-m\int^v M/Nv'dv'} \times\int \frac{ve^{m\int^v M/Nv'dv'}(-\int^v(S-s)v'^2dv'+C_1)}{N}dv, \tag{60}$$

already shown elsewhere.[11,12]

In Fig. 5 we contrast the initial α velocity V_α to plasma thermal velocities in term of temperature. It is obvious that inequalities (1) on which results derived in Sec. III are based are satisfied only at high temperature. Present solutions are free from this drawback because they do not have to rely on inequalities (1).

Now, it is instructive to focus on a few specific cases.

A. Particular cases

When $T_e=T_i\equiv T$, expression (60) is simplified to

$$f(v)=\frac{m}{T}e^{-(mv^2/2T)} \times\int \frac{ve^{mv^2/2T}}{M}\left(-\int^v(S-s)v'^2dv'+C_1\right)dv. \tag{61}$$

It is also often convenient to put loss term s under the form $s=\kappa v^\sigma$, with $\kappa=0$, $v\gg v_\alpha$, so that

$$f(v)=\frac{m}{T}e^{-(mv^2/2T)}\int\frac{ve^{mv^2/2T}}{M} \times\left(-\int^v Sv'^2dv'+\frac{\kappa v^{\sigma+3}}{\sigma+3}+C_1\right)dv \tag{62}$$

can fulfill the second boundary condition. As far as S is concerned, Eq. (61) may then be further simplified by neglecting initial velocities of the fusioning particles while maintaining the view that α particles are produced with velocity v_α. So, the source term reduces to the unnormalized equivalent of expression (50),

$$S=\frac{\dot{n}_\alpha}{4\pi v_\alpha^2}\,\delta(v-v_\alpha), \tag{63}$$

which v-quadrature fulfills the two boundary conditions when $C_1=0$, and one obtains the simplified stationary distribution

$$f(v)=\frac{m}{T}e^{-(mv^2/2T)}\int\frac{v e^{mv^2/2T}}{M}\times\left(\frac{n_\alpha}{4\pi}\,\theta(v_\alpha-v)+\frac{\kappa v^{\sigma+3}}{\sigma+3}\right)dv. \tag{64}$$

However, it is also possible to retain the complete S expression (13), which thus yields

$$\begin{aligned}I&=-\int S(v)v^2dv\\&=-\frac{\dot{n}_\alpha}{8\sqrt{2}\pi^{3/2}v_\alpha}\Bigg(2v_{Ti}\{e^{-[(v+v_\alpha)^2/2v_{Thi}^2]}\\&\quad-e^{-[(v-v_\alpha)^2/2v_{Thi}^2]}\}+\sqrt{2}\pi v_\alpha\\&\quad\times\left\{\phi\left(\frac{v-v_\alpha}{\sqrt{2}v_{Thi}}\right)+\phi\left(\frac{v+v_\alpha}{\sqrt{2}v_{Thi}}\right)\right\}\Bigg),\end{aligned} \tag{65}$$

fulfilling boundary conditions with

$$C_1=\frac{\dot{n}_\alpha}{4\pi}$$

in a more realistic distribution

$$f(v)=\frac{m}{T}e^{-(mv^2/2T)}\int\frac{v e^{mv^2/2T}}{M}\left(I+\frac{\dot{n}_\alpha}{4\pi}+\frac{\kappa v^{\sigma+3}}{\sigma+3}\right)dv. \tag{66}$$

Other options remain open for the loss term s.

Focusing attention on the most energetic α_s', one can neglect thermalized ones. As above, one thus discounts particles with a velocity smaller than a velocity slightly larger than v_{Thi},

$$s=0,\quad v>v_{\text{cutoff}}=\frac{3v_{Thi}}{2}. \tag{67}$$

More generally, one may take an arbitrarily small v_{cutoff} which simplifies Eq. (66) even further to

$$f(v)=\frac{m}{T}e^{-(mv^2/2T)}\int\frac{v e^{mv^2/2T}}{M}\left(I+\frac{\dot{n}_\alpha}{4\pi}\right)dv. \tag{68}$$

It is also meaningful to explain s in terms of the α particles residence time τ with

$$s=\frac{f}{\tau}, \tag{69}$$

and the stationary FPE,

$$0=\sum_\beta\frac{C_\beta}{v^2}\frac{\partial}{\partial v}\left(\phi_{1\beta}f+\frac{T_\beta}{m}\frac{\phi_{1\beta}}{v}\frac{\partial f}{\partial v}\right)+S-\frac{f}{\tau}. \tag{70}$$

Integrating once more Eq. (70), yields

$$Mf+\frac{N}{m}\frac{1}{v}\frac{\partial f}{\partial v}=-\int Sv^2dv+\frac{1}{\tau}\int fv^2dv, \tag{71}$$

which provides an approximate solution when the second quadrature on the right-hand side is performed at zero loss ($\tau\to\infty$), yielding the isotropic expression

$$f_{\tau\to\infty}(v)=\frac{m}{T}e^{-(mv^2/2T)}\times\int\frac{v e^{mv^2/2T}}{M}\left(-\int^v Sv'^2dv'+C_1\right)dv, \tag{72}$$

which may be explained further through the density of α particles with velocities between 0 and V, as

$$n_{\tau\to\infty}(v)\equiv 4\pi\int_0^v f_{\tau\to\infty}v'^2dv'. \tag{73}$$

B. Connection to usual solutions

It is now appropriate to compare the present results to the previous formulation (52) valid when inequalities (1) hold. We retrieve it in our more general formulation by putting $s=0$ or by retaining losses for nonthermalized α_s' in the stationary FPE (70).[18–22]

The opposite limits of low and high velocity are, respectively, highlighted through

$$\phi_1(x)=\phi(x)-x\frac{\partial\phi(x)}{\partial x}$$

with ($u=bv$),

$$\begin{aligned}&\phi_1(u)=\frac{4}{\sqrt{\pi}}\sum_{n=0}^{\infty}(-1)^n\frac{u^{2n+3}}{(2n+3)n!},\quad u\ll 1,\\&\phi_1(u)\to 1-\frac{e^{-u}}{\sqrt{\pi}}\left[2u+\frac{1}{u}+\sum_{n=0}^{\infty}(-1)^n\frac{1.3\cdots(2n-1)}{2^n u^{2n+1}}\right],\quad u\gg 1,\end{aligned} \tag{74}$$

and coefficients C_β (collision time τ_e),

$$C_e=\frac{3\sqrt{\pi}}{\eta b^3\tau_e},\quad C_i=\frac{3\sqrt{\pi}}{\eta\gamma b^3\tau_e},\quad\text{where}\quad \eta=\frac{m}{m_e}.$$

So, the FPE expression (70) becomes

$$0=\frac{3\sqrt{\pi}}{4u^2}\frac{\partial}{\partial u}\left(M^*F+\frac{M^*}{2\eta u}\frac{\partial F}{\partial u}\right)+S, \tag{75}$$

with

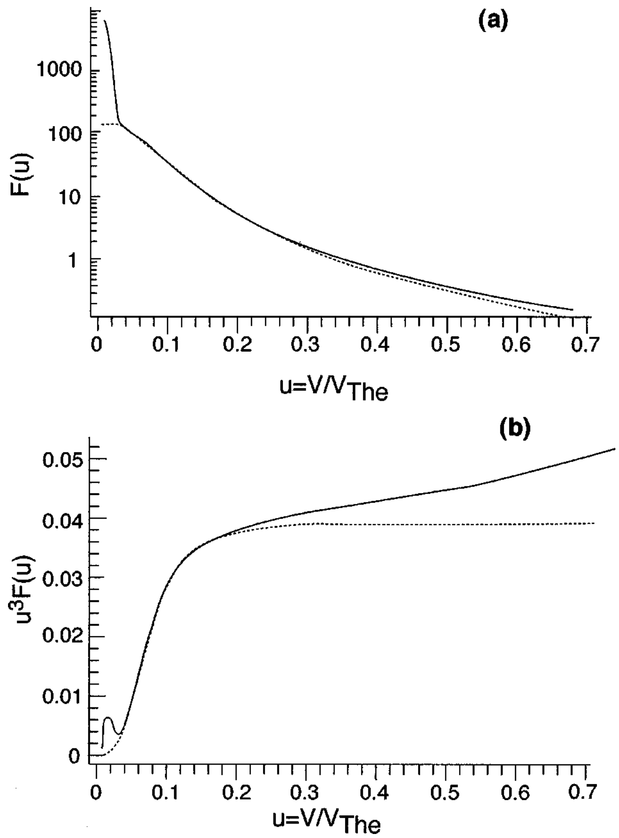

FIG. 6. (a) Exact distribution $F(u)$ (78) (continuous line) compared to the standard expression (52) (dotted line); (b) corresponding $u^3F(u)$. $T=T_e=T_i=1$ keV.

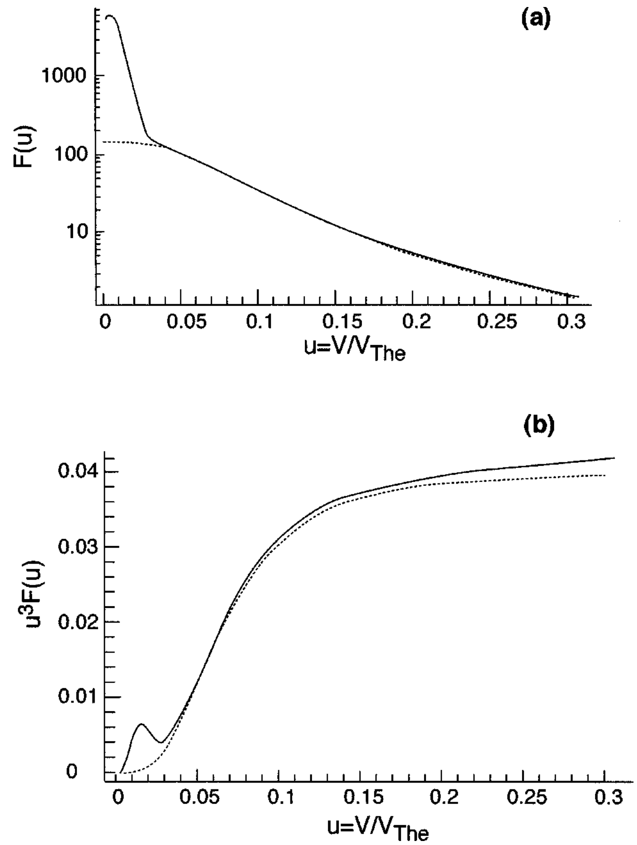

FIG. 7. Same caption as in Figs. 4. $T=5$ keV.

$$M^*=\phi_1(u)+\frac{\phi_1(\sqrt{\gamma}u)}{\gamma}, \tag{76}$$

the sum of the electron and ion contributions. Restricting to the first term in expansions (74), one can already work out a rather efficient solution through the simple approximants

$$\phi_1(u)\cong pu^3, \quad u\ll 1,$$

$$\phi_1(u)\cong 1, \quad u\gg 1,$$

yielding $M^*\cong pu^3+(1/\gamma)$. Then, neglecting $(1/2\eta u)\times(\partial F/\partial u)/F$ to comply with inequalities (1), allows us to reshape Eq. (75) under the form

$$0\cong 3F+u\left(1+\frac{3\sqrt{\pi}}{4\gamma u^3}\right)\frac{\partial F}{\partial u}+S, \tag{77}$$

equivalent to Eq. (48) already derived previously[13,14] from Braginski coefficients.[16] In this connection, it is useful to recognize that for a deltalike S [cf. Eq. (50)] and same loss s as above, the normalized velocity distribution obtained in Sec. III A may be written as

$$F(u)=\frac{\eta\gamma\theta(u_\alpha-u)}{3\pi^{3/2}}e^{-\eta u^2}\int\frac{ue^{\eta u^2}}{\gamma\phi_1(u)+\phi_1(\sqrt{\gamma}u)}du. \tag{78}$$

In Figs. 6–9, we therefore compare the standard result (52) to our general expression (78). We consider α particles with an initial 3.5 MeV kinetic energy. Ion mass is taken as average of D and T. In Figs. 6(a) and 7(a) one can see that some discrepancy remains in the high velocity limit. This is due to the fact that in the few keV temperature range, $v\cong v_{The}$, and the second inequality (1) cannot hold. At higher plasma temperature T, this mismatch decreases inversely with increasing T. As demonstrated in Figs. 6(b)–9(b), those discrepancies exhibit similar trends for the $F(u)$ cubic moment,

$$\langle v\rangle=\int vf(v)d^3v=\frac{1}{b^4}\int uF(u)4\pi u^2du, \tag{79}$$

which is relevant to the velocity average.

Also, V_{cutoff} has been chosen very small in order to include the low v values for thermalized particles. Then $v\leqslant v_{Thi}$, and F derivative is not small compared to F, so inequalities (1) are no longer valid in this regime, which explains the huge discrepancy in Figs. 6(a)–9(a) for very small u. The corresponding u range is shown to increase with T. Another remarkable feature is the nearly T-independence of the normalized distribution $F(u)$. Those calculations demonstrate the capabilities of the present general expression for $F(u)$ to account self-consistently for v- and T-variations on a large scale.

It also proves instructive to combine the approximants given below Eq. (76) into the simple Padé[13] expression

$$\phi_{1a}(u)\approx\frac{pu^3}{1+pu^3}, \quad p=\frac{4}{3\sqrt{\pi}}, \quad \text{all } u, \tag{80}$$

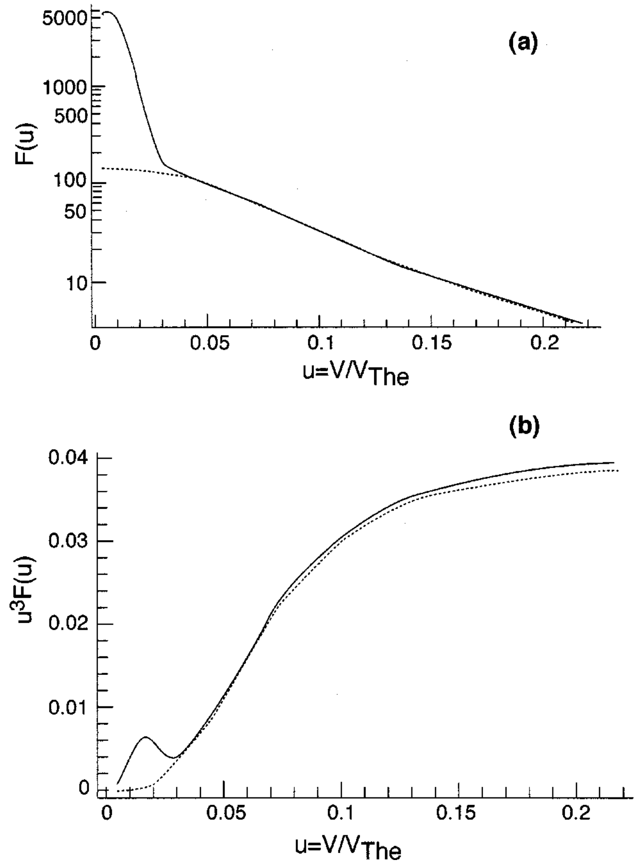

FIG. 8. Same caption as in Figs. 4. $T=10$ keV.

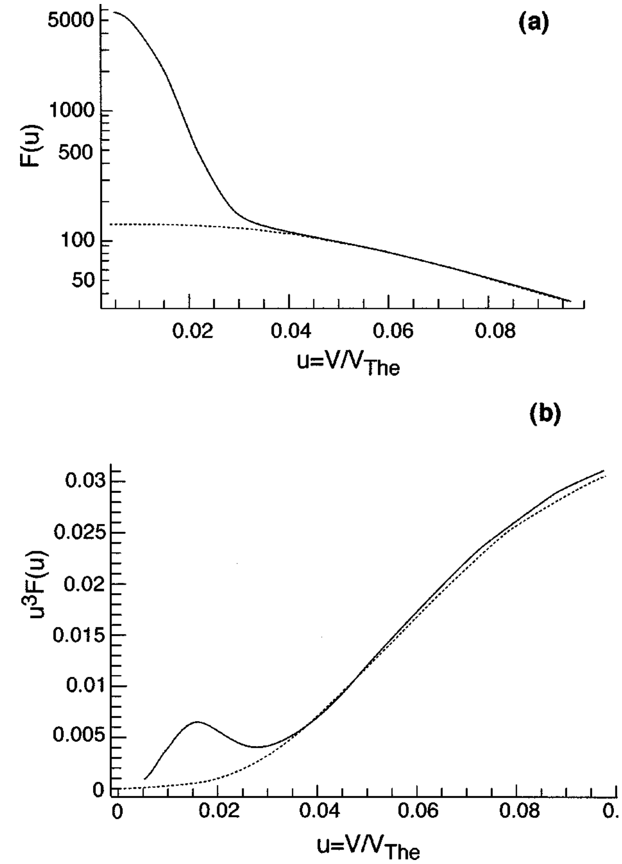

FIG. 9. Same caption as in Figs. 4. $T=50$ keV.

contrasted accurately in Fig. 10 to its fully computed counterpart. ϕ_{1a} introduced into Eq. (78) then provides a precise and quasianalytic approximation to $F(u)$ given as

$$F_0(u)=\frac{\eta\gamma\theta(u_\alpha-u)}{3\pi^{3/2}}e^{-\eta u^2}\int\frac{ue^{\eta u^2}}{\gamma\phi_1(u)+\phi_1(\sqrt{\gamma u})}du. \tag{81}$$

When $v\geqslant v_{Thi}$, $\phi_1(\sqrt{\gamma u})$ turns negligible relative to the corresponding collision contribution. So, Eq. (81) reduces to

$$\begin{aligned}F_0(u)&=\frac{\eta\theta(u_\alpha-u)}{3\pi^{3/2}p}e^{-\eta u^2}\int\frac{ue^{\eta u^2}(1+pu^3)}{u^3}du\\&\cong\frac{\eta\theta(u_\alpha-u)}{3\pi^{3/2}p}e^{-\eta u^2}\left\{\left(\frac{p}{2\eta}-\frac{1}{u}\right)e^{\eta u^2}\right.\\&\quad\left.+\sqrt{\pi\eta}\phi_i(\sqrt{\eta u})\right\},\end{aligned} \tag{82}$$

with $\phi_1(x)=i\phi(ix)$. This approximation is plotted in Fig. 11 with a full numerical $F(u)$ evaluation. Agreement is rather convincing for $v\geqslant 10\,v_{Thi}$, at any plasma temperature.

V. TIME-DEPENDENT FPE

The macroscopic plasma electric field is assumed negligible. So, the general FPE expression,

$$\begin{aligned}&\frac{\partial f}{\partial t}+v\cdot\frac{\partial f}{\partial\mathbf{r}}+\frac{q}{m}(v\times\mathbf{B})\cdot\frac{\partial f}{\partial v}\\&\quad=\sum_\beta\frac{C_\beta}{v^2}\frac{\partial}{\partial v}\left(\phi_{1\beta}f+\frac{T_\beta}{m}\frac{\phi_{1\beta}}{v}\frac{\partial f}{\partial v}\right)+S-s,\end{aligned} \tag{83}$$

simplifies to

$$\frac{\partial f}{\partial t}+v\cdot\frac{\partial f}{\partial\mathbf{r}}=\sum_\beta\frac{C_\beta}{v^2}\frac{\partial}{\partial v}\left(\phi_{1\beta}f+\frac{T_\beta}{m}\frac{\phi_{1\beta}}{v}\frac{\partial f}{\partial v}\right)+S-s, \tag{84}$$

for a v-isotropic f distribution with plasma dependence $f=f(v,n(\mathbf{r},t),T(\mathbf{r},t),t)$ in density and temperature. The

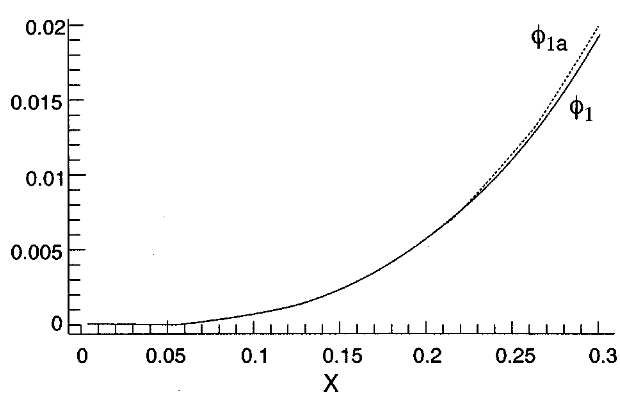

FIG. 10. Exact ϕ_1 function and its Padé ratio approximant ϕ_{1a} (80).

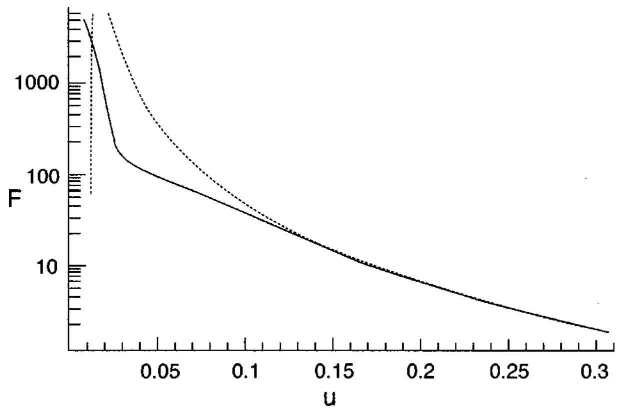

FIG. 11. Full equilibrium distribution (78) (continuous line) for thermonuclear α particles and its approximation (82) (dotted line) $T=5$ keV, $u_\alpha=0.308$.

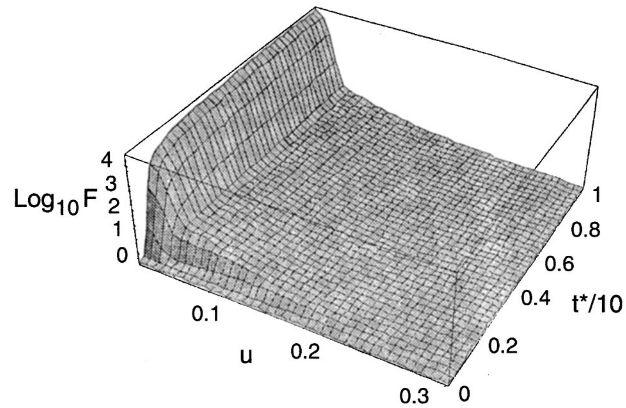

FIG. 12. Temporal evolution of the α distribution ($E_\alpha=3.5$ MeV), plasma temperature $T=5$ keV$\Rightarrow u_\alpha=0.308$.

plasma is assumed in local thermodynamic equilibrium (LTE). Then, space derivatives may be neglected when $L \gg l_{\mathrm{MFP}}^{i,e}$ is fulfilled. We also assume that the density of produced α_s' is sufficiently low to preclude any significant perturbation in the LTE plasma. This restriction implies that thermonuclear reaction rate remains far below that of the number of already produced α_s'. Then, kinetic Eq. (84) may be reformulated as

$$\frac{df}{dt}=\sum_\beta \frac{C_\beta}{v^2}\frac{\partial}{\partial v}\left(\phi_{1\beta}f+\frac{T_\beta}{m}\frac{\phi_{1\beta}}{v}\frac{\partial f}{\partial v}\right)+S-s, \tag{85}$$

with α particles generated through the time-independent source term S (37).

At $t=0$, no α has yet shown up, so we have $f(v,t=0)=0$, boundary condition to add to previous ones,

$$f(v_l,t)=0, \quad v_l \gg v_\alpha, \qquad \left.\frac{\partial f(v,t)}{\partial v}\right|_{v=0}=0. \tag{86}$$

Going back to the FPE standard treatment (Sec. III), one can straightforwardly write down the given t-extension as

$$\frac{\partial f}{\partial t}\cong 3f+\left(v+\frac{v_c^3}{v^2}\right)\frac{\partial f}{\partial v}+\frac{S_{\tau\alpha e}}{2}-\frac{f}{\tau}, \tag{87}$$

which, by putting[6] $S=0$ (no source), yields the approximation

$$\frac{\partial f}{\partial t}\cong 3f+\left(v+\frac{v_c^3}{v^2}\right)\frac{\partial f}{\partial v}-\frac{f}{\tau}. \tag{88}$$

Imposing above boundary conditions does not automatically lead to an obvious analytic solution in Eq. (87). So, Liberman–Velikovich[13] proposed another boundary condition,

$$f(v\to v_\alpha,t)\to \frac{\dot n_\alpha \tau_{\alpha e}\theta(v_\alpha-v)}{8\pi(v^3+v_c^3)}, \tag{89}$$

imposing the t-dependent solution to reproduce the stationary one for $v\sim v_\alpha$, initial α velocity. The resulting simplified FPE upon introduction of a new variable,

$$\xi=2\int_0^t \frac{dt'}{\tau_{\alpha e}(t')}$$

yields

$$f(v,t)=\exp\left(3\xi-\int_0^\xi \frac{\tau_{\alpha e}(\xi')d\xi'}{\tau}\right)g(v,\xi), \tag{90}$$

with the g function to be further explained.

Also Kolesnichenko[12] proposed a general expression

$$f(v,t)=y_1(v)t+y_2(v),$$

which does not fit the above initial condition at $t=0$, below Eq. (85).

Facing those difficulties, we found it useful to proceed to a numerical solution of the normalized function of time $F \equiv f/\dot n_\alpha \tau_{\alpha e} b^3$ with normalized velocity u and normalized t^*,

$$t^*\equiv \frac{t}{\tau_{\alpha e}}.$$

So, the above equation reads as

$$\frac{\partial F}{\partial t^*}=\frac{3\sqrt{\pi}}{4u^2}\frac{\partial}{\partial u}\left(M^*F+\frac{M^*}{2\eta u}\frac{\partial F}{\partial u}\right)+S-s, \tag{91}$$

with a normalized source term

$$S(u)=\frac{n_\alpha b^3\sqrt{\gamma}}{4\pi^{3/2}u_\alpha u}\{e^{-\gamma(u-u_\alpha)^2}-e^{-\gamma(u+u_\alpha)^2}\}, \tag{92}$$

and a loss term in the form

$$s=\frac{F}{\tau^*}, \tag{93}$$

where $s=0$, $v>v_{\mathrm{cutoff}}$, $v_{\mathrm{cutoff}}=0.0001$.

Figure 12 displays the corresponding distribution. In order to account for thermalized α_s', one has chosen $v_{\mathrm{cutoff}}=0.0001$.

Those results agree quantitatively to former ones derived for other plasma densities and temperatures with an unormalized distribution.

F gets stabilized at a time nearly twice the energy exchange time $\tau_{\alpha e}$. When S and s are t-independent, manifestly this stable state is in equilibrium. Figure 12 demonstrates how the distribution relaxes to equilibrium through friction and diffusion.

At equilibrium, $t_{\rm eq} \sim 2\tau_{\alpha e}$ F stays in a permanent stationary state. According to Cozzani–Horton,[14] a general necessary and sufficient condition for this phenomenon to occur writes as

$$\int_V d^3r \int S(v) d^3v = \int_V d^3r \int s(v) d^3v. \tag{94}$$

Integration volume V has to satisfy $V \gg l_{\rm MFP}^3$, i.e., the number of produced α_s' should just compensate for the number of lost ones in V. This relationship gets fulfilled when $v_{\rm cutoff} < v < v_\alpha$. Corresponding analytic and stationary distribution is the LTE. It writes as

$$f(v) = \frac{m}{T} e^{-(mv^2/2T)} \int \frac{v e^{(mv^2/T)}}{M} \left(I + \frac{\dot{n}_\alpha}{4\pi} \right) dv. \tag{95}$$

$t_{\rm eq}$ gets shorter when $v_{\rm cutoff}$ increases, altogether with losses. Specifying the FPE (91) when losses rely on F and residence time τ, one obtains ($\tau^* = \tau/\tau_{\alpha e}$)

$$\frac{\partial F}{\partial t^*} = \frac{3\sqrt{\pi}}{4u^2} \frac{\partial}{\partial u} \left(M^* F + \frac{M^*}{2\eta u} \frac{\partial F}{\partial u} \right) + S - \frac{F}{\tau^*}, \tag{96}$$

so $t_{\rm eq}$ also depends on τ. Corresponding accurate numerical F values are displayed in Figs. 13.

If $\tau \gg t_{\rm eq}$ with $t_{\rm eq}$ determined through cutoff losses ($t_{\rm eq} \cong 2\tau_{\alpha e}$, $u_{\rm cutoff} \ll 1$), equilibrium is reached nearly at same time. On the other hand, when $\tau \ll \tau_{\alpha e}$, relaxation to equilibrium proceeds much more rapidly. Figure 13(a) demonstrates that $t_{\rm eq} \cong 1.5\,\tau_{\alpha e}$ and the maximum of the thermalized edge of the distribution becomes ten times smaller.

In Fig. 13(b), τ turns even shorter altogether with corresponding $t_{\rm eq}$. The ridge maximum of the Maxwell thermalized part is now shrinked by another 30 factor.

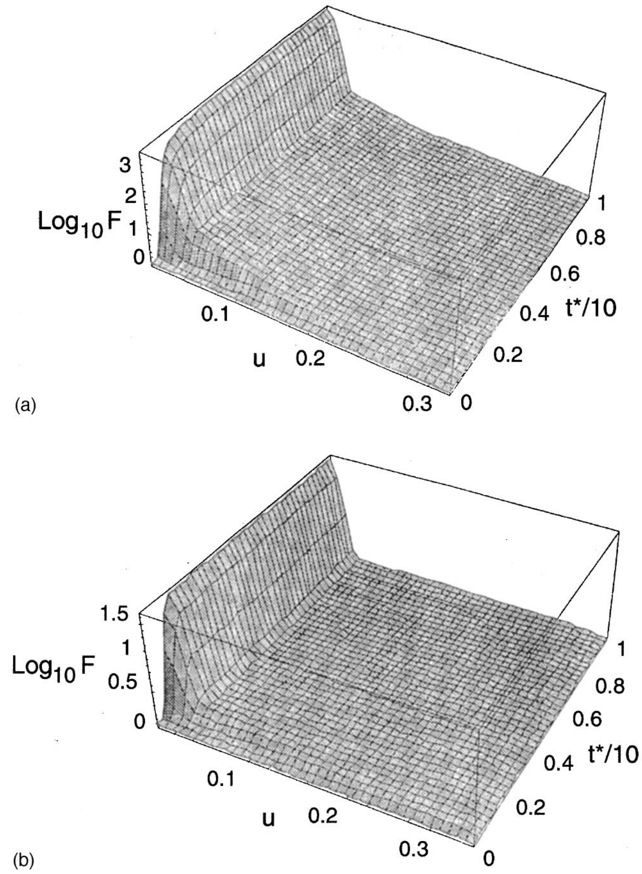

FIG. 13. Same caption as in Fig. 12. (a) Residence time $\tau = \tau_{\alpha e}$; (b) residence time $\tau = 0.2\,\tau_{\alpha e}$.

VI. RELAXATION TOWARD EQUILIBRIUM

Relaxation mechanisms can be straightforwardly extrapolated from previous calculations by selecting a much longer residence time $\tau = 5\tau_{\alpha e}$, for the α particles in plasma. Just born α_s' appear first distributed around the mean creation velocity v_α [Fig. 14(a)]. Stopping mechanisms have not yet taken their toll on the initial $E_\alpha = 3.5$ MeV. The distribution function then retains the shape of source term S, which gets nearly linearly amplified with increasing time. During next time interval [Fig. 14(b)], F reaches equilibrium, at least for particles with $v \geq$ initial mean velocity. Corresponding α_s' lose energy mostly through electron collisions. Then, the number of low energy particles steadily increases. In Fig. 14(b), near the end of time interval, the lowest particles also lose energy through collisions with plasma ions. F then starts increasing for $u \sim 0$. When $0.3 \leq t^* \leq 1.5$ [Fig. 14(c)], F gets to equilibrium through electron collisions, for nearly every α particle. Finally [Fig. 14(d)], turns stabilized at equilibrium for very low thermalized v values.

VII. F MAGNETIC CORRECTIONS

Up to now, we avoided any direct implication of the imposed magnetic intensity B on the distribution F. Our elaboration rested essentially on the isotropic source term S, yielding a isotropic zero-order approximation for the α particles distribution. Moreover, we restricted to a strong magnetization albeit limited so that $\omega_c < \omega_p$. Electron gyroradius ρ_{Le} thus remains much larger than corresponding Debye length λ_D. So, the β-deflections of particle trajectories within a screening sphere are hardly noticeable (Sec. III).

Nonetheless, to validate conceptually and quantitatively this approach, we have now to pay attention to higher order manifestations of the magnetic field. Those are expected to show up as a linear superposition of magnetic and collisional corrections to zero-order F. One gets them through the FPE,

$$\frac{df}{dt} = \frac{\partial f}{\partial t} + v \cdot \frac{\partial f}{\partial \mathbf{r}} + \frac{q}{m} (\mathbf{v} \times \mathbf{B}) \cdot \frac{\partial f}{\partial \mathbf{v}} = C(f) + S - s, \tag{97}$$

with B-free collision coefficients,

$$C(f) = -\sum_i \frac{\partial}{\partial v_i} \left(a_i f - d_{ij} \frac{\partial f}{\partial v_j} \right),$$

when $\lambda_D \ll \rho_{Le}$ altogether with $\omega_c \ll \omega_p$. Then, upon introducing the perturbative dichotomy $f = f_0 + \epsilon_1 \delta f$ with relevant smallness parameter $\epsilon_1 = \lambda_D/\rho_{Le} = (\omega_c/\sqrt{2}\omega_p) \ll 1$ so that $\epsilon_1 \delta f \ll f_0$ one first retrieves f_0 FPE,

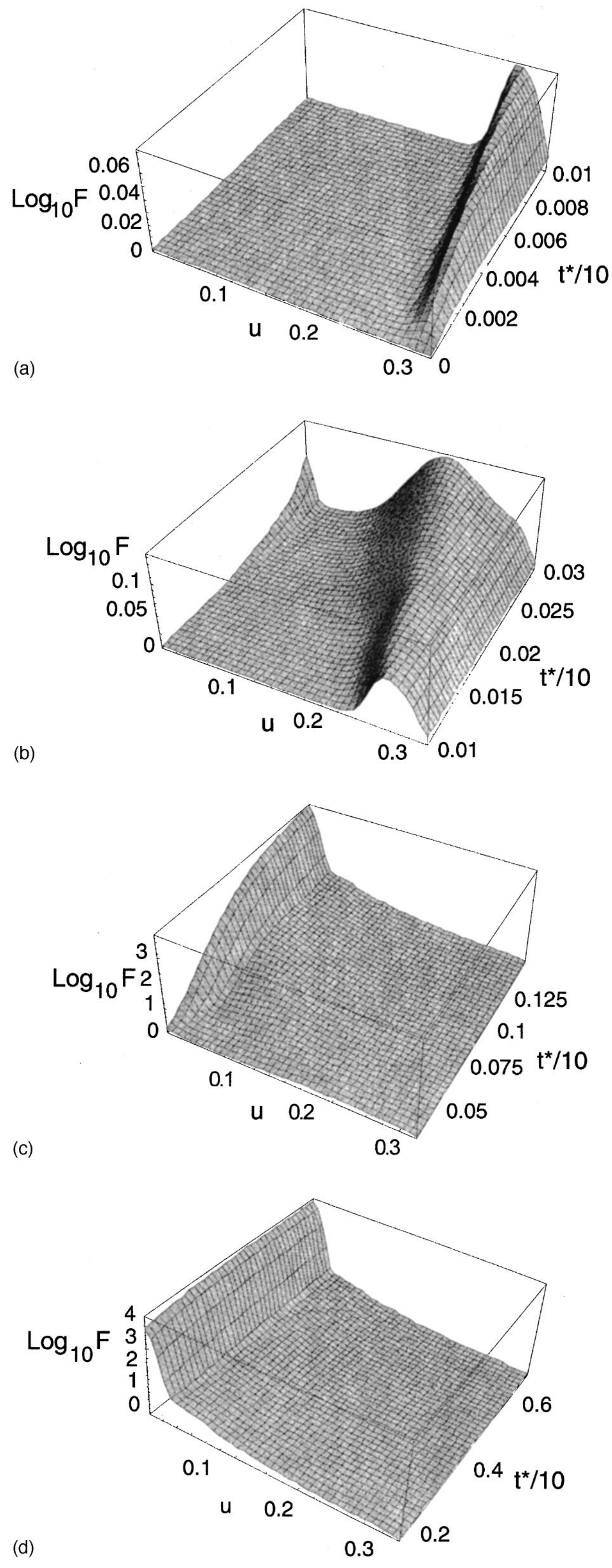

FIG. 14. Production of thermonuclear α particles, in a plasma at $T = 5$ keV, with residence time $\tau = 5\ \tau_{\alpha e}$. (a) Initial stage without α-stopping by target electrons; (b) α stopping through target electron collisions. Equilibrium is reached. The number of slower α_s' colliding with target ions steadily increases. (c) Same caption as in (b) at later times; (d) equilibrium is finally obtained at very low velocities for thermalized α_s'.

$$0 = C(f_0) + S - s, \tag{98}$$

with solution (37) under condition (94), for a v-isotropic f_0 so that $(\mathbf{v}\times\mathbf{B})\cdot\partial f_0/\partial\mathbf{v} = 0\cdot\epsilon_1\partial f$ then fulfills

$$\frac{\partial(f_0+\epsilon_1\delta f)}{\partial t} + v\cdot\frac{\partial(f_0+\epsilon_1\delta f)}{\partial\mathbf{r}} + \epsilon_1\omega_c(\mathbf{v}\times\hat{\mathbf{b}})\cdot\frac{\partial\delta f}{\partial\mathbf{v}} = \epsilon_1 C(\delta f), \tag{99}$$

in terms of gyrofrequency $\omega_c = qB/m$ and unit vector $\hat{\mathbf{b}} = \mathbf{B}/B$. Keeping track of full time dependence $\delta f = \delta f(v, n(\mathbf{r},t), T(\mathbf{r},t))$ with partial derivatives

$$\frac{1}{T}\frac{\partial T}{\partial t} = -\frac{1}{c_v}\nabla_r\cdot\mathbf{v},$$

$$\frac{1}{p}\frac{\partial p}{\partial t} = -\frac{c_p}{c_v}\nabla_r\cdot\mathbf{v},$$

and recalling that in a monatomic plasma fluid[16] one has $\nabla_r\cdot\mathbf{v} = \mathbf{0}$, so that $\partial f/\partial t = 0$, $\epsilon_1\delta f$ is given by

$$\mathbf{v}\cdot\frac{\partial(f_0+\epsilon_1\delta f)}{\partial\mathbf{r}} + \epsilon_1\omega_c(\mathbf{v}\times\hat{\mathbf{b}})\cdot\frac{\partial\delta f}{\partial\mathbf{v}} = \epsilon_1 C(\delta f). \tag{100}$$

In view of times inequality $\tau_1 \ll \tau_0$, one can safely neglect plasma compression rate, and consider it uncompressible. f may then be determined through local space–time values of hydrodynamic quantities.

So, we are led to introduce the scaled transformations $r \equiv LR$ with $L \gg l_{\mathrm{MFP}}$ and $v \equiv U(v)$ in terms of mean quadratic velocity. So, Eq. (100) becomes

$$\frac{\langle\mathbf{v}\rangle}{L\omega_c}\mathbf{U}\cdot\frac{\partial(f_0)}{\partial\mathbf{R}} + \frac{\langle\mathbf{v}\rangle}{L\omega_c}\epsilon_1\mathbf{U}\cdot\frac{\partial\delta\mathbf{f}}{\partial\mathbf{R}}\epsilon_1(\mathbf{U}\times\hat{\mathbf{b}})\cdot\frac{\partial\delta f}{\partial\mathbf{U}} = \frac{\epsilon_1}{\omega_c}C(\delta f), \tag{101a}$$

with a negligible second term $\sim\epsilon_1$, in the left-hand side because of

$$\frac{\langle\mathbf{v}\rangle}{L\omega_c} = \frac{\langle\mathbf{v}\rangle\rho_L}{Lv_\perp} \sim \frac{\rho_L}{L} \equiv \epsilon_0 \ll 1 \tag{101b}$$

with

$$\rho_L \ll l_{\mathrm{MFP}} \ll L.$$

So, one is left with

$$\frac{\mathbf{v}}{\omega_c}\cdot\frac{\partial f_0}{\partial\mathbf{r}} + \epsilon_1(\mathbf{v}\times\hat{\mathbf{b}})\cdot\frac{\partial\delta f}{\partial\mathbf{v}} = \frac{\epsilon_1}{\omega_c}C(\delta f), \tag{102}$$

which may be simplified further with the highly plausible assumption $\omega_c \gg \nu$. Actually, for the MTF parameters (Sec. I) of the present concern, one has

$$3.3\times10^{-5} \leq \frac{\nu}{\omega_c} \leq 3.3\times10^{-3}.$$

So, one can split the searched high order corrections into a superposition of collisionless magnetic contribution with an additional weakly collisional one.

A. Weakly collisional plasmas

In this framework, it appears appropriate to notice that

$$C(f)=\nu\hat{C}(f)$$

may be introduced in Eq. (78) with

$$\frac{\mathbf{v}}{\omega_c}\cdot\frac{\partial f_0}{\partial \mathbf{r}}+\epsilon_1(\mathbf{v}\times\hat{\mathbf{b}})\cdot\frac{\partial \delta f}{\partial \mathbf{v}}=\epsilon_1\frac{\nu}{\omega_c}\hat{C}(\delta f), \tag{103}$$

and a negligible right-hand side at order ϵ_1, in view of the above assumption

$$\epsilon_2\equiv\frac{\nu}{\omega_c}\ll 1$$

yielding

$$\epsilon_1\epsilon_2=\frac{\omega_c}{\sqrt{2}\,\omega_p}\,\frac{\nu}{\omega_c}=\frac{\nu}{\sqrt{2}\,\omega_p}\ll\frac{\omega_c}{\sqrt{2}\,\omega_p}=\epsilon_1 .$$

So, the final equation pertinent at that order now reads as

$$\frac{\mathbf{v}}{\omega_c}\cdot\frac{\partial f_0}{\partial \mathbf{r}}+(\mathbf{v}\times\hat{\mathbf{b}})\cdot\frac{\partial(\epsilon_1\delta f)}{\partial \mathbf{v}}=0, \tag{104}$$

fulfilled by

$$\epsilon_1\delta f_1=\frac{1}{\omega_c}\mathbf{v}\cdot\hat{\mathbf{b}}\times\cdot\nabla_r f_0 \tag{105}$$

as easily checked by direct substitution into Eq. (104) when using vectorial relationships

$$\frac{1}{\omega_c}\mathbf{v}\cdot\nabla_r f_0+\frac{1}{\omega_c}(\mathbf{v}\times\hat{\mathbf{b}})\cdot\frac{\partial}{\partial \mathbf{v}}(\mathbf{v}\cdot\hat{\mathbf{b}}\times\nabla_r f_0)=0,$$

$$(\mathbf{v}\cdot\hat{\mathbf{b}})(\hat{\mathbf{b}}\cdot\boldsymbol{\nabla}_r f_0)=0.$$

Last equality implies that plasma spatial gradients are kept orthogonal to $\mathbf{B}$ with $\boldsymbol{\nabla}_r=\boldsymbol{\nabla}_\perp$, $\boldsymbol{\nabla}_\perp\perp\hat{\mathbf{b}}$, so that transport quantities computed $\|\mathbf{B}$ retain their field-free values.

B. Collision effects

Collision contribution is now considered as a second order approximation $\epsilon_2\delta f_2$ on $\epsilon_1\delta f$. Total magnetic corrections thus appear as a linear superposition

$$\epsilon_1\delta f=\epsilon_1\delta f_1+\epsilon_2\delta f_2$$

with

$$\epsilon_2\delta f_2\ll\epsilon_1\delta f_1 .$$

Then, inserting expression (105) for $\epsilon_1\delta f_1$ in Eq. (103) produces

$$\frac{\mathbf{v}}{\omega_c}\cdot\frac{\partial f_0}{\partial \mathbf{r}}+\epsilon_1(\mathbf{v}\times\hat{\mathbf{b}})\cdot\frac{\partial \delta f_1}{\partial \mathbf{v}}+\epsilon_2(\mathbf{v}\times\hat{\mathbf{b}})\cdot\frac{\partial \delta f_2}{\partial \mathbf{v}}$$
$$=\frac{1}{\omega_c}C(\epsilon_1\delta f_1)+\epsilon_2^2\hat{C}(\delta f_2). \tag{106}$$

Taking into account that

$$\frac{\mathbf{v}}{\omega_c}\cdot\frac{\partial f_0}{\partial \mathbf{r}}+\epsilon_1(\mathbf{v}\times\hat{\mathbf{b}})\cdot\frac{\partial \delta f_1}{\partial \mathbf{v}}=0,$$

Eq. (101b) may be rewritten as

$$\epsilon_2(\mathbf{v}\times\hat{\mathbf{b}})\cdot\frac{\partial \delta f_2}{\partial \mathbf{v}}=\frac{1}{\omega_c}C(\epsilon_1\delta f_1)+\epsilon_2^2\hat{C}(\delta f_2), \tag{107}$$

while neglecting the quadratic contribution $\sim\epsilon_2^2$. One thus arrives at

$$(\mathbf{v}\times\hat{\mathbf{b}})\cdot\frac{\partial(\epsilon_2\delta f_2)}{\partial \mathbf{v}}=\frac{1}{\omega_c}C(\epsilon_1\delta f_1), \tag{108}$$

$$-\frac{1}{\omega_c^2}C(\mathbf{v}\cdot\hat{\mathbf{b}}\times\nabla_\perp f_0)+(\mathbf{v}\times\hat{\mathbf{b}})\cdot\frac{\partial(\epsilon_2\delta f_2)}{\partial \mathbf{v}}=0. \tag{109}$$

From $\lambda_D\ll\rho_L$, one infers that collision terms do not rely on B. By symmetry with Eq. (106), solutions of Eqs. (108)–(109) should have the form[23]

$$\begin{aligned}\epsilon_2\delta f_2&=\frac{-1}{\omega_c^2}C(\mathbf{v}\cdot\hat{\mathbf{b}}\times(\hat{\mathbf{b}}\times\nabla_\perp f_0)),\\&=\frac{1}{\omega_c^2}C(\mathbf{v}\cdot\boldsymbol{\nabla}_\perp f_0).\end{aligned} \tag{110}$$

In this connection, it should be noticed that Lifschitz–Pitaevski[23] already obtained expressions (105) and (110) by using different methods.

C. Nonisotropic distribution

Within the FPE framework, one can also address the issue of a nonisotropic α distribution when collisions with Maxwellian plasma particles are envisioned.

Adapting straightforwardly Sec. III notations the collision term on the plasma particules appears as ($\beta=e,i$ pertains to plasma particles)

$$C(f)=-\sum_{\beta,i}\frac{\partial}{\partial v_i}\left(a_i\delta f-d_{ij}\frac{\partial f}{\partial v_j}\right), \tag{111}$$

with friction vector

$$a_i=-\frac{4\pi n_\beta L}{m m_\beta v^3}\left(\frac{q q_\beta}{4\pi\epsilon_0}\right)^2\phi_1(b_\beta v)v_i$$

and diffusion tensor

$$v_j d_{ij}=-\frac{m_\beta}{m2b_\beta^2}a_i .$$

In this context, close to tokamak physics, it is useful to introduce spherical coordinates.[24]

Switching from tensor to vector flux divergence in velocity space, one can thus write

$$\sum_i\frac{\partial j_i}{\partial v_i}=\frac{\partial}{\partial \mathbf{v}}\cdot\mathbf{j}=\boldsymbol{\nabla}_v\cdot\mathbf{j}$$

in spherical coordinates. Friction is obviously $\|\mathbf{v}$, while friction tensor turns diagonal in a coordinate system with axis $\|\mathbf{v}$, $\mathbf{v}$ being the velocity of α particles with a given distribution. So, we get

$$\frac{\partial}{\partial \mathbf{v}}\cdot\mathbf{j}=\frac{1}{v^2}\frac{\partial}{\partial v}(v^2 j_{\parallel})+\frac{1}{\mu\sin\theta}\frac{\partial}{\partial\theta}(\sin\theta j_{\perp})+\frac{1}{\mu\sin\theta}\frac{\partial}{\partial\varphi}(j_{\perp}) \qquad (112)$$

with flux components[8,17]

$$\mathbf{j}_{\parallel}=af-d_{\parallel}\nabla_{v\parallel}f,$$

$$\mathbf{j}_{\perp}=-d_{\perp}\nabla_{v\perp}f,$$

where

$$a=-\frac{4\pi n_\beta L}{m m_\beta v^2}\left(\frac{qq_\beta}{4\pi\epsilon_0}\right)^2\phi_1(b_\beta v),$$

$$d_{\parallel}=\frac{2\pi n_\beta L}{m^2 v}\left(\frac{qq_\beta}{4\pi\epsilon_0}\right)^2\frac{\phi_1(b_\beta v)}{(b_\beta v)^2},$$

$$d_{\perp}=\frac{2\pi n_\beta L}{m^2 v}\left(\frac{qq_\beta}{4\pi\epsilon_0}\right)^2\left(\phi(b_\beta v)-\frac{\phi_1(b_\beta v)}{(b_\beta v)^2}\right).$$

Choosing the z axis along the distribution spatial gradient so that $f=\mathbf{v}\cdot\nabla_{\perp}f_0-v\nabla_{\perp}f_0\cos\theta$, allows us to express flux components in velocity space in the form

$$\mathbf{j}_{\perp}=-\frac{d_{\perp}}{v}\frac{\partial}{\partial\theta}(v\nabla_{\perp}f_0\cos\theta)=d_{\perp}\nabla_{\perp}f_0\sin\theta,$$

$$\frac{1}{v\sin\theta}\frac{\partial}{\partial\theta}(\sin\theta j_{\perp})=\frac{2d_{\perp}\nabla_{\perp}f_0\cos\theta}{v}, \qquad (113)$$

$$\mathbf{j}_{\parallel}=\left\{av\nabla_{\perp}f_0-d_{\parallel}\frac{\partial}{\partial v}(v\nabla_{\perp}f_0)\right\}\cos\theta.$$

Finally, the second order contribution may be given as

$$\delta f_2=\frac{1}{\omega_2}\frac{\cos\theta}{v^2}\frac{\partial}{\partial v}\left(v^2\left\{av\nabla_{\perp}f_0-d_{\parallel}\frac{\partial}{\partial v}(v\nabla_{\perp}f_0)\right\}\right)+\frac{2d_{\perp}\nabla_{\perp}f_0\cos\theta}{\omega_c^2 v}, \qquad (114)$$

with implicit β-summation over plasma species.

VIII. VELOCITY MOMENTS

Once α particles distribution is known, its v^n-moments give access to many equilibrium and transport quantities of fundamental concern.

A. Particle density

First v-moment involves the density of created α particles

$$n(\mathbf{r},t)=\int f(\mathbf{r},\mathbf{v},t)d^3v. \qquad (115)$$

At equilibrium, this quadrature specializes to

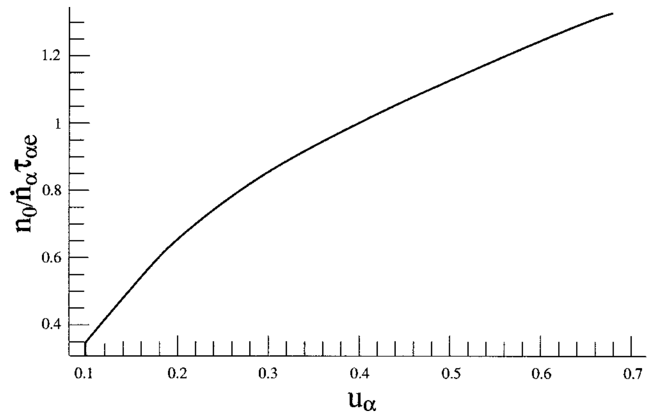

FIG. 15. Normalized density of thermonuclear α particles in a plasma with $1\leqslant T\leqslant 50$ keV with an initial creation speed $v_\alpha=1.3\times10^9$ cm/s.

$$n_0=4\pi\int_0^\infty f_0(v)v^2dv$$

$$=\frac{4\pi m}{T}\int_0^\infty dv\,v^2e^{-(mv^2/2T)}\int_0^v dv'\times\frac{v'e^{-(mv'^2/2T)}}{M}\left(I+\frac{\dot{n}_\alpha}{4\pi}\right)$$

$$=4\pi\dot{n}_\alpha\tau_{\alpha e}\int_0^\infty F_0(u)u^2du. \qquad (116)$$

The second line implies a residence time much longer than that for energy exchange with a loss term featuring

$$v_{\text{cutoff}}\ll v_{Thi}.$$

The normalized version (third line) acknowledges that when T varies, the only relevant variable is the normalized creation speed $u_\alpha=v_\alpha\sqrt{m_e/2T}$.

Corresponding results are thus visualized in Fig. 15 for plasma temperatures $1\leqslant T\leqslant 50$ keV. They are rather interpolated with the approximant

$$\frac{n_0}{\dot{n}_\alpha\tau_{\alpha e}}\cong a+bu_\alpha^c,$$

where $a=-1.7294$, $b=3.3046$, and $c=0.2037$.

B. Equilibrium mean energy

It is important to know the mean energy of produced α_s' after relaxation to equilibrium by colliding with plasma particles. Most significant contribution to energy exchange arises from nonthermal particles. Then, using equilibrium distribution (95) allows us to obtain the mean energy of nonthermalized particles under the form

$$\langle E\rangle_{\text{nonth}}=\left\langle\frac{mv^2}{2}\right\rangle_{\text{nonth}}=\frac{\int\frac{mv^2}{2}f_0(v)d^3v}{n_0}\cong\frac{2\pi m}{n_0}\int_{v_{Thi}}^\infty v^4f_0(v)dv. \qquad (117)$$

For instance, varying T (keV) between 4 and 6 yields $\langle E\rangle_{\rm nonth}$ (MeV) between 0.25 and 0.265, which amounts to $\langle E\rangle_{\rm nonth}\cong E_\alpha/14$, with E_α, initial α_s' kinetic energy.

So, those particles deliver $\langle E_{\rm yield}\rangle\cong 13E_\alpha/14 \cong 2.25$ MeV per particle to the target plasma, when particle losses are assumed negligible.

C. Particle flux

At order f_0, the flux of the thermonuclear particles

$$\Gamma=n\langle\mathbf{v}\rangle=\int\mathbf{v}f(v)d^3v, \tag{118}$$

vanishes. First, the nonzero contribution is due to $\epsilon_1\delta f_1$ [cf. Eq. (105)]. It is given as ($\epsilon_1=1$),

$$\Gamma_1=\int\mathbf{v}\delta f_1 d^3v=\frac{1}{\omega_e}\hat{\mathbf{b}}\times\nabla_\perp\int\mathbf{v}\cdot\mathbf{v}f_0d^3v$$
$$=\frac{2}{m\omega_e}\hat{\mathbf{b}}\times\nabla_\perp\left\langle\frac{1}{2}mv^2\right\rangle n_0, \tag{119}$$

with n_0, α particles density. Putting $\frac{1}{2}mv^2\equiv\frac{3}{2}T_{\rm eff}$, Eq. (95) becomes

$$\Gamma_1=\frac{2}{m\omega_e}\hat{\mathbf{b}}\times\nabla_\perp\left(\frac{3}{2}T_{\rm eff}n_0\right)=\frac{3}{m\omega_e}\hat{\mathbf{b}}\times\nabla_\perp p, \tag{120}$$

for an equilibrium plasma taken as a perfect gas ($p=nT$). Then, comparing Γ_1 to diffusion equation $\Gamma=\overline{D}\nabla n_0$ yields a first order diffusion coefficient

$$\overline{D}_1=\frac{3}{m\omega_c}b_k\epsilon_{ijk}=\frac{3}{qB}b_k\epsilon_{ijk}, \tag{121}$$

with antisymmetric tensor ϵ_{ijk}.

Selecting orientation $\mathbf{B}\|o\mathbf{x}$, one can specify $\overline{D}_1$ as

$$\overline{D}_1=\frac{3}{m\omega_c}\begin{pmatrix}0&0&0\\0&0&-1\\0&1&0\end{pmatrix}.$$

The given particle flux is then orthogonal to the magnetic field and pressure spatial gradient. It decreases for increasing B values and obviously depends on particle charge sign.

The second order contribution (110) ($\epsilon_2=1$) yields

$$\Gamma_2=\int\mathbf{v}\epsilon_2\delta f_2d^3v=\frac{1}{\omega_c^2}\int\mathbf{v}C(\mathbf{v}\cdot\nabla_\perp f_0)d^3v, \tag{122}$$

a much more involved expression. It may then be explained as

$$\Gamma_2=2\pi\int dv\int_0^\pi v\cos\theta\delta f_2v^2\sin\theta d\theta\hat{\mathbf{k}}$$
$$=-\frac{4\pi}{3\omega_c^2}\int_0^\infty dv\,v^3\left[\frac{1}{v^2}\frac{\partial}{\partial v}(v^2j_\parallel^*)+\frac{2d_{\perp\beta}\nabla_\perp f_0}{v}\right]\mathbf{k}, \tag{123}$$

with

$$j_\parallel^*=a_\beta v\nabla_\perp f_0-d_{\parallel\beta}\frac{\partial}{\partial v}(v\nabla_\perp f_0).$$

This expression $\sim B^{-2}$ remains parallel to spatial gradient. It results from a combination of magnetic field and collisions in a nonhomogeneous plasma.

Assuming $\nabla_\perp T=0$, one can through

$$f_0\equiv f_0(v,T(\mathbf{r}),n(\mathbf{r}))$$

and

$$\nabla_\perp f_0=\frac{\partial f_0}{\partial T}\nabla_\perp T+\frac{\partial f_0}{\partial n}\nabla_\perp n$$

rewrite Eq. (123) as

$$\Gamma_2=-\frac{4\pi}{3n\omega_c^2}\sum_\beta\int_0^\infty dv\left[v\frac{\partial}{\partial v}\right.$$
$$\left.\times(v^2\{a_\beta vf_0-d_{\parallel\beta}(vf_0)\})+2d_{\perp\beta}\nabla_\perp f_0v^2\right]\nabla_\perp n_0. \tag{124}$$

Putting altogether first order contribution (121) and second order contribution (124), yields the diffusion tensor expression

$$\overline{D}=\overline{D}_1+D_2\mathbf{I}=\frac{3}{m\omega_c}b_k\epsilon_{ijk}-\frac{4\pi}{3n\omega_c^2}\sum_\beta\int_0^\infty dv\left[v\right.$$
$$\times\frac{\partial}{\partial v}(v^2\{a_\beta vf_0-d_{\parallel\beta}(vf_0)\})$$
$$\left.+2d_{\perp\beta}\nabla_\perp f_0v^2\right]\mathbf{I}. \tag{125}$$

D. Heat flux

Corresponding heat (energy) flux expression is given by

$$\mathbf{q}=\int\mathbf{v}Ef(v)d^3v=\int\mathbf{v}\frac{1}{2}mv^2f(v)d^3v, \tag{126}$$

with a first order contribution

$$\mathbf{q}_1=\frac{m}{2}\int\mathbf{v}v^2\delta f_1(v)d^3v$$
$$=\frac{m}{2\omega_c}\hat{\mathbf{b}}\times\nabla_\perp\int\mathbf{v}\cdot\mathbf{v}v^2f_0d^3v$$
$$=\frac{2}{m\omega_c}\hat{\mathbf{b}}\times\nabla_\perp(n_0\langle E^2\rangle)\equiv\overline{\kappa}_1\nabla_\perp T_{\rm eff} \tag{127}$$

orthogonal to $\mathbf{B}$ and conductivity thermal tensor

$$\overline{\kappa}_1=\frac{9n_0T_{\rm eff}}{m\omega_c}b_\kappa\epsilon_{ijk}. \tag{128}$$

Second order contribution, parallel to spatial gradient reads as

$$\mathbf{q}_2 = \int \mathbf{v} E\,\delta f_2 d^3 v$$
$$= \frac{m\pi}{\omega_c^2}\int dv \int_0^\pi v\cos\theta v^2 \delta f_2 v^2 \sin\theta d\theta \hat{\mathbf{k}}$$
$$= -\frac{2m\pi}{3\omega_c^2}\sum_\beta \int_0^\infty dv\left[v^3\frac{\partial}{\partial v}(v^2 j_\parallel^*) + 2d_{\perp\beta}\nabla_\perp f_0 v^4\right]\hat{\mathbf{k}}. \tag{129}$$

Retaining the $\nabla_\perp T$ contribution in $\nabla_\perp f_0$, provides the second-order heat flux contribution,

$$\mathbf{q}_2 = -\frac{2m\pi}{3\omega_c^2}\sum_\beta \int_0^\infty dv\left[v^3\frac{\partial}{\partial v}\left(v^2\left\{a_\beta v\frac{\partial f_0}{\partial T} - d_{\parallel\beta}\frac{\partial}{\partial v}\left(v\frac{\partial f_0}{\partial T}\right)\right\}\right) + 2d_{\perp\beta}\frac{\partial f_0}{\partial T}v^4\right]\nabla_\perp T. \tag{130}$$

So, the complete thermal conductivity tensor is

$$\overline{\kappa} = \overline{\kappa_1} + \kappa_2 \mathbf{I} = \frac{9n_0 T_{\rm eff}}{m\omega_c} b_\kappa \epsilon_{ijk} - \frac{2m\pi}{3\omega_c^2}\sum_\beta \int_0^\infty dv\left[v^3\frac{\partial}{\partial v}\left(v^2\left\{a_\beta v\frac{\partial f_0}{\partial T} - d_{\parallel\beta}\frac{\partial}{\partial v}\left(v\frac{\partial f_0}{\partial T}\right)\right\}\right) + 2d_{\perp\beta}\frac{\partial f_0}{\partial T}v^4\right]\mathbf{I}, \tag{131}$$

and it is practical to re-explain the coefficients detailed below Eq. (112) in the form

$$a_\beta = \frac{3\sqrt{\pi}m_e}{\eta b^3 \tau_e m_\beta}\phi_1(b_\beta v),$$
$$d_{\parallel\beta} = \frac{3\sqrt{\pi}m_e}{2\eta b^3\tau_e m}\frac{\phi_1(b_\beta v)}{(b_\beta v)^2}, \tag{132}$$
$$d_{\perp\beta} = \frac{3\sqrt{\pi}m_e}{2\eta b^3\tau_e m}\left(\phi(b_\beta v) - \frac{\phi_1(b_\beta v)}{(b_\beta v)^2}\right),$$

in terms of plasma collision time τ_e.

At first order, the above quantities behave $\sim B^{-1}$ through $D_1 \propto 1/\omega_c$ and $\kappa_1 \propto 1/\omega_c$, for instance.

Equilibrium distribution f_0 for Maxwellian plasma particles does not rely on τ_e. So, their second-order contribution behave as $D_2 \propto 1/\omega_c^2\tau_e$ and $\kappa_2 \propto 1/\omega_c^2\tau_e$. Such a behavior is at variance with that advocated by Braginski,[16] which reads as

$$\kappa \propto \frac{1}{\Delta}, \quad \Delta = \delta_0 + \delta_1(\omega_c\tau_e)^2 + (\omega_c\tau_e)^4$$

with B- and ν-independent δ_0 and δ_1 coefficients.

Present behaviors also depart from Liberman–Velikovich[13] scaling with $\kappa_1 \propto 1/\omega_c\tau_e$.

Present results are compatible with Lifschitz–Pitaevsky methodology[23] highlighting a dominant magnetic contribution valid when $\omega_c \gg \nu$. On the other hand, other authors[13,16] stress strong collisional effects. We think that the present approach is more suitable to plasmas encountered in magnetized target fusion (MTF).

IX. SUMMARY

We have proceeded to a thorough examination of the Fokker–Planck formalism for the distribution function of α-particles in a thermonuclear DT plasma envisioned in the scenario of magnetized target fusion with a cylindrical target. Such a plasma is dense and strongly magnetized and it fulfills $\omega_c \gg \nu$.

So, it is possible to work out a general stationary FPE solution which may be initialized as isotropic in velocity space, in terms of isotropic source and loss terms.

The basic results given in Sec. IV are novel ones. They are valid in a much wider velocity and temperature range than those proposed earlier.[13,14]

They allow the further inclusion of temporal dependence as well as higher order magnetic and collisional contributions to the velocity distribution of α particles. Relaxation to equilibrium has also been considered. Velocity moments of the new stationary distribution provide access to particle and heat transport, with a scaling in τ_e different from that one in tokamak plasmas where $\rho_L \leqslant \lambda_D$.

In conclusion, those fundamental kinetic-theoretic results should prove significant to increase our knowledge of the MTF and Z pinches[25] plasmas, as well.

ACKNOWLEDGMENTS

It is our pleasure to thank Professors Gérard Leclerc, Jacques Misguich, and Dr. Boris Weyssow for a highly fruitful interaction leading to many improvements.

One of us (C.C.) is also grateful to CONICIT-Caracas (Venezuela) for awarding a grant during his doctoral stay at Orsay.

[1] See, for instance, R. E. Siemon, I. R. Lindemuth, and K. F. Schoenberg, Comments Plasma Phys. Control. Fusion **18**, 363 (1999).
[2] R. C. Kirkpatrick and I. R. Lindemuth, in *Current Trends in International Fusion Research*, edited by E. Panarella (Plenum, New York, 1997), p. 319.
[3] M. A. Sweeney and A. V. Farnsworth, Jr., Nucl. Fusion **21**, 41 (1981).
[4] I. R. Lindemuth and R. C. Kirkpatrick, Nucl. Fusion **23**, 263 (1983).
[5] R. D. Jones and W. C. Mead, Nucl. Fusion **26**, 127 (1986).
[6] R. C. Kirkpatrick, I. R. Lindemuth, and M. S. Ward, Fusion Technol. **27**, 201 (1995).
[7] M. D. Churazov, B. Yu Sharkov, and E. A. Zabrodina, Fusion Eng. Des. **32–33**, 577 (1996).
[8] M. D. Churazov, A. G. Aksenov, N. A. Krasnoborov, and E. A. Zabrodina, Nucl. Instrum. Methods Phys. Res. A **415**, 144 (1998).
[9] M. Basko, A. Kemp, and J. Meyer-ter-Vehn, Nucl. Fusion **40**, 59 (2000).
[10] J. Wesson, *Tokamaks* (Clarendon, Oxford, 1987).
[11] D. C. Montgomery, L. Turner, and G. Joyce, Phys. Fluids **17**, 954 (1974); **17**, 2201 (1974).
[12] Ya. I. Kolesnichenko, Nucl. Fusion **20**, 727 (1980); Sov. J. Plasma Phys. **1**, 442 (1975).
[13] M. Liberman and A. Velikovich, J. Plasma Phys. **31**, 369 (1984).
[14] F. Cozzani and W. Horton, J. Plasma Phys. **36**, 313 (1986).
[15] D. Sivukhin, *Reviews of Plasma Physics* (Consultants Bureau, New York, 1966), Vol. 4; R. Liboff, *Introduction to the Kinetic Theories* (Wiley, New York, 1969).
[16] S. Braginskii, *Reviews of Plasma Physics* (Consultants Bureau, New York, 1966), Vol. 1.
[17] L. Hinton and D. Hazeltine, Rev. Mod. Phys. **48**, 239 (1076).
[18] C. Cereceda, M. de Peretti, and M. Sabatier, *Strongly Coupled Coulomb Systems*, edited by G. J. Kalman, J. M. Rommel, and K. Blagoev (Plenum, New York, 1998), p. 543.

[19]C. Cereceda, Ph.D. thesis, Université Paris XI, Orsay, 15 Mars, 1999 (unpublished).
[20]P. Martin and G. Baker, J. Math. Phys. **32**, 1470 (1991).
[21]H. Saito, T. Sekiguchi, M. Katsurai, and S. Maekawa, Nucl. Fusion **17**, 919 (1977).
[22]H. Tsuji, M. Katsurai, T. Sekiguchi, and N. Nakano, Nucl. Fusion **16**, 287 (1976).
[23]E. Lifschitz and L. Pitaevsky, *Course of Theoretical Physics* (Pergamon, Oxford, 1981), Vol. 10.
[24]M. Lisak, D. Anderson, H. Hamnen, H. Wilhelmsson, and M. Tendler, Nucl. Fusion **22**, 515 (1982).
[25]See, for instance, T. W. L. Sanford, R. C. Mock, R. B. Spielman, D. L. Peterson, D. Mosher, and N. F. Roderick, Phys. Plasmas **5**, 3755 (1998).